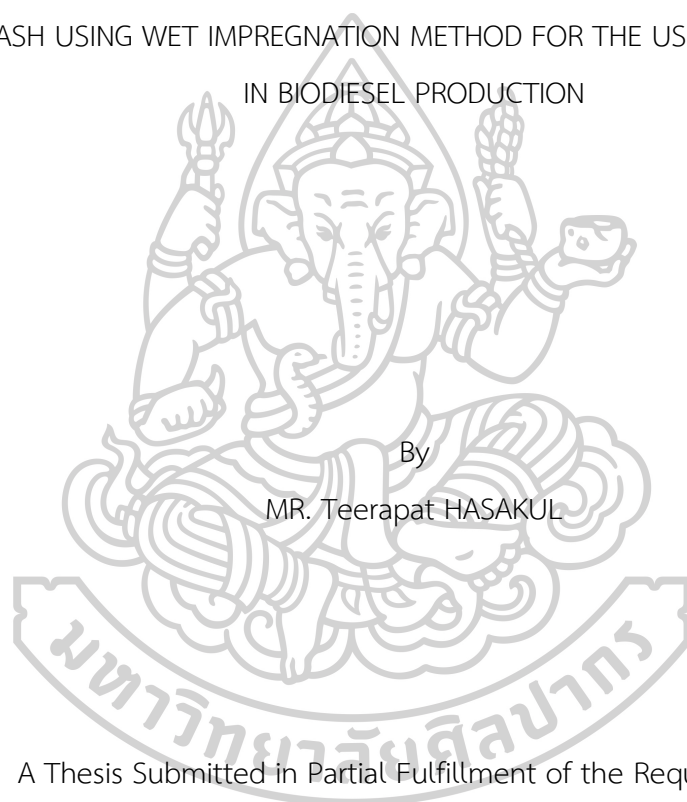THE STUDY ON THE PREPARATION OF TRISODIUM PHOSPHATE-IMPREGNATED ON
BOTTOM ASH USING WET IMPREGNATION METHOD FOR THE USE AS THE CATALYSTS
IN BIODIESEL PRODUCTION

By

MR. Teerapat HASAKUL

A Thesis Submitted in Partial Fulfillment of the Requirements

for Master of Engineering (CHEMICAL ENGINEERING)

Department of CHEMICAL ENGINEERING

Graduate School, Silpakorn University

Academic Year 2020

Copyright of Graduate School, Silpakorn University

การศึกษาไตรโซเดียมฟอสเฟตที่ถูกตรึงบนเถ้าหนักด้วยวิธีเอิบชุ่มสำหรับใช้เป็นตัวเร่ง
ปฏิกิริยาในการผลิตน้ำมันไบโอดีเซล

โดย
นายธีรภัทร ห้าสกุล

วิทยานิพนธ์นี้เป็นส่วนหนึ่งของการศึกษาตามหลักสูตรวิศวกรรมศาสตรมหาบัณฑิต
สาขาวิชาวิศวกรรมเคมี แผน ก แบบ ก 2 ระดับปริญญามหาบัณฑิต
ภาควิชาวิศวกรรมเคมี
บัณฑิตวิทยาลัย มหาวิทยาลัยศิลปากร
ปีการศึกษา 2563

THE STUDY ON THE PREPARATION OF TRISODIUM PHOSPHATE-
IMPREGNATED ON BOTTOM ASH USING WET IMPREGNATION METHOD FOR
THE USE AS THE CATALYSTS IN BIODIESEL PRODUCTION

By

MR. Teerapat HASAKUL

A Thesis Submitted in Partial Fulfillment of the Requirements

for Master of Engineering (CHEMICAL ENGINEERING)

Department of CHEMICAL ENGINEERING

Graduate School, Silpakorn University

Academic Year 2020

Copyright of Graduate School, Silpakorn University

Title   The Study on the Preparation of Trisodium phosphate-impregnated
             on Bottom Ash using Wet Impregnation Method for the Use as the
             Catalysts in Biodiesel Production
By   Teerapat HASAKUL
Field of Study   (CHEMICAL ENGINEERING)
Advisor   Sunthon Piticharoenphun , Ph.D.

Graduate School Silpakorn University in Partial Fulfillment of the Requirements for the Master of Engineering

....Dean of graduate school
(Associate Professor Jurairat Nunthanid, Ph.D.)

Approved by

....Chair person
(Assistant Professor Tarawipa Puangpetch , Ph.D.)

....Advisor
(Sunthon Piticharoenphun , Ph.D.)

....Co advisor
(Dussadee Rattanaphra , D.Eng.)

....Committee
(Associate Professor Prakorn Ramakul , D.Eng.)

....External Examiner
(Associate Professor Unchalee Suwanmanee , Ph.D.)
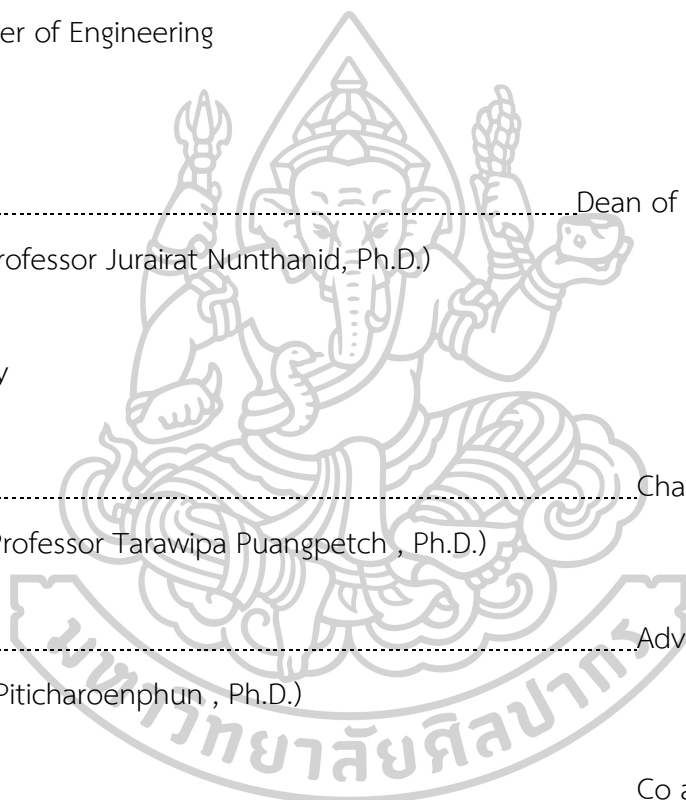
61404208 : Major (CHEMICAL ENGINEERING)

Keyword : Coal bottom ash, trisodium phosphate, Biodiesel, Transesterification, Box-Behnken

MR. TEERAPAT HASAKUL : THE STUDY ON THE PREPARATION OF TRISODIUM PHOSPHATE-IMPREGNATED ON BOTTOM ASH USING WET IMPREGNATION METHOD FOR THE USE AS THE CATALYSTS IN BIODIESEL PRODUCTION THESIS ADVISOR : SUNTHON PITICHAROENPHUN, Ph.D.

This work aimed to study the preparation of trisodium phosphate impregnated on bottom ash using wet impregnation method for use as the catalyst in transesterification reaction. Both coal bottom ash and trisodium phosphate were wastes or by-products from the combustion and Thai monazite ore separation, respectively. The catalyst was characterized using BET, CO_2-TPD, XRD, and XRF techniques. The results from XRD showed that coal bottom ash consisted of quartz and mullite (mostly Si and Al). The various synthesis conditions were investigated such as trisodium phosphate (TSP) loadings, impregnation temperatures, and calcination temperatures. TSP loadings were varied at 10, 20, 30 and 40 wt%. The impregnation temperatures were carried out at room temperature (25 °C), 40, 60 and 80 °C, and the calcination temperatures were studied at 150, 250, 350 and 450 °C. The results showed that the highest %FAME of 90.26% was observed when using the catalyst which was impregnated using TSP loading of 40% at the impregnation temperature of 60 °C and the calcinations temperature of 350 °C. The %FAME strongly depended on the basicity of catalyst. Higher basicity of catalyst provided more activities of catalyst in transesterification reaction. In addition, the Box-Behnken experimental design was used in this work to study the interaction between variables and responses. The trend of %FAME result using Box-Behnken corresponded to the results from the study of various conditions mentioned previously. The optimum conditions of catalyst synthesis were observed using Minitab optimizer, which were TSP loading of 40 wt%, impregnation temperature of 80 °C and calcination temperature of 278 °C.

Furthermore, the suitable ratio of methanol to oil and the reusability were studied. The suitable ratio of methanol to oil was 18:1. After the reaction, the catalyst was washed with methanol several times to reuse in the transesterification reaction. It showed that the reusability of catalyst was not observed due to the loss of active sites and the deactivation of the catalyst.
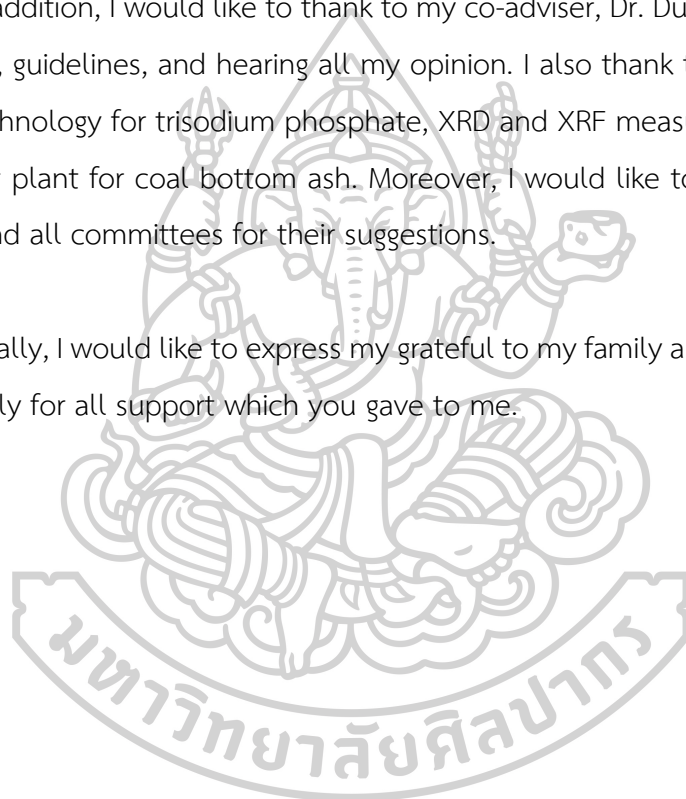
ACKNOWLEDGEMENTS

TABLE OF CONTENTS

Chapter 1 Introduction

This chapter mentions the motivation of this research which gives explanation about biodiesel, bottom ash and trisodium phosphate. The objectives and scopes of the research are also described. Lastly, the benefits of this research are stated in the last section.

1.1 Motivation

1.1.1 Biodiesel

Nowadays, the amount of fossil fuel is considerably decreasing due to high consumption. Therefore, it is necessary to carry out the research about alternative energy for energy security in the future. In Thailand, the alternative energy can be divided into 3 groups. The first group is electricity which is produced from solar, wind, dam, coal power plant and etc. The second group is heat which is generated from solar, waste, biomass and etc. The last group is biofuels which are manufactured from ethanol, biodiesel, pyrolysis oil, and etc. [1]. Biodiesel is considerably interesting from many researchers in Thailand because Thailand can provide several sources of raw material to produce biodiesel, such as palm, soybean, coconut and jatropha. In addition, these raw materials are cheap and abundant. As raw materials used for biodiesel production are from natural sources, it is also beneficial for agriculture section in Thailand.

For the problem about air pollution, the hot issue at the present in Thailand is "PM 2.5". PM 2.5 is produced from many routes, such as burning in the open air, industries, transportation, electricity generation and household. In Europe, diesel engine is the main reason for producing PM 2.5 [2]. It was observed that the fossil fuel source caused this PM 2.5 problem. In contrast, the many researches indicated that

biodiesel was cleaner energy than fossil diesel from petroleum source because biodiesel emission produced less amount of PM 2.5 [3]. Therefore, Thai government supports the use of biodiesel as one of alternative energy sources, especially from the palm biodiesel. This can help the palm planters to increase palm trading and also the use of palm biodiesel can reduce the air pollution such as PM 2.5.

The well-common processes for biodiesel production are contributed into 2 processes. The first process is esterification reaction. The esterification reaction uses free fatty acid and alcohol as raw materials and uses acids as the catalyst. However, this reaction takes a long reaction time and high temperature. The second process is transesterification reaction. This reaction uses fatty acid and alcohol as raw materials but uses bases as the catalyst. Anyway, it takes the shorter time for reaction. However, transesterification reaction is not suitable to be used for the raw material which contains a lot of acid and water [4]. At high content of acid and water, the side reaction which is saponification reaction can occur. The saponification reaction produces soaps which can reduce the yield of biodiesel production. In addition, it is difficult to separate soaps from biodiesel. The separation uses the large amount of water to leach soaps out from biodiesel. Therefore, the soap separation generates a lot of wastewater which need to be treated before discharge, increasing biodiesel production cost.

In case of the use of homogeneous catalyst, the separation of catalyst from the product is the main problem which increases the cost of biodiesel production. From this problem, the heterogeneous catalyst is likely to be suitable catalyst in biodiesel production. It is also easier to separate the heterogeneous catalyst out of the product and then the catalyst can be reused several times. This help to reduce the cost of catalyst and help to decrease wastewater, leading to lower cost of biodiesel production.

At present, there are several researches studying the use of heterogeneous catalysts in transesterification reaction for biodiesel production. Therefore, this

research aims to study the preparation of heterogeneous catalyst which provide high efficiency and low cost for biodiesel production.

1.1.2 Bottom ash

In Thailand, the trend of energy consumption is continually increasing. The main reason of higher energy consumption is the growth of industrial section and transportation. There are several energy resources for energy usage in Thailand, such as natural gas, water and coal [5]. The energy from coal power plant is one of energy resource which supports the security of energy consumption in Thailand. The benefit of the use of coal is that energy production cost is low and it can provide adequate amount of energy at high consumption, including Thailand has some types of coals in the nature by its own [6]. Therefore, many coal powers plants have been located in different parts of Thailand such as BLCP power plant in Rayong, Glow SPP 3 in Rayong, GHECO-One power plant, National power supply, Mae Moh power plant and so on [7]. Different types of raw materials can be used in a power plant for steam production such as bituminous, lignite, sub-bituminous, peat and anthracite [8]. For example, BLCP power plant and Glow CFB 3 use bituminous, while 'Mae Moh' power plant uses lignite as raw material.

It was estimated that 40,000 ton per day of coal was used to generate energy. As the result, a large amount of coal ash was obtained from the coal combustion process. Coal ash can be classified into two types; fly ash and bottom ash. Fly ash from coal combustion, which is not heavy, is mixed with hot gas, flowing to the top of the boiler furnace. Then, the fly ash is separated using electrostatic precipitator. For bottom ash, its weight is heavier than fly ash. Thus, bottom ash falls down to the bottom part of combustion tower. The amount of total coal ash was approximately 10,000 ton per day. This can be roughly distributed into 6,000 ton of fly ash and 4,000 ton of bottom ash. As a large amount of both fly and bottom ash is obtained from combustion process, they can be used in many applications. Fly ash and bottom ash

can be used to mix with the concrete to reduce the cost of construction [9, 10]. Especially, the cost of dam construction, which is paid for a great amount of concrete, can be reduced from the use of the mixture between concrete and fly ash (Rolling Compact concrete) [11]. Some research found the use of coal bottom ash as a coarse binder in mortar that improve the strength of mortar mixture [12]. In addition, fly ash and bottom ash are composed of SiO_2, Al_2O_3, CaO and Fe_2O_3 in its composition [9]. Therefore, fly ash and bottom can be used as the catalyst in many reactions, such as oxidation of toluene to produce benzoic acid, hydrogenolysis of glycerol for propanediol production, Friedel-Crafts acylation reaction and Knoevenagel condensation [13]. The use of bottom ash as the catalyst was found in air gasification of palm kernel shell, biomass gasification, pyrolysis for syngas, and in dye-degradation as the support of catalyst [14-16]. It has not been found that the bottom ash was used as the catalyst for biodiesel production. This might be that it contained less active site for transesterification reaction. However, some work showed that the bottom ash can offer high surface area which can be loaded an active compound, providing a great amount of active sites [14]. Due to the great amount of bottom ash generated from combustion process in the power plant, most of bottom ash was sold with the cheap price to be used as the mixture of concrete. To add more value of bottom ash, this research chose to study the use of bottom ash as the supporter of a catalyst for transesterification reaction in biodiesel production.

1.1.3 Trisodium phosphate

Trisodium phosphate is an organic compound of which its melting point is at 1,340 °C. It is in the form of powder with the density of 2.536 g/cm^3 (at 17.5 °C), and soluble in water [17]. Trisodium phosphate has basic site and provides reusability [18]. The application of trisodium phosphate is found in laxative, electrolyte replacement purposes and dietary supplement [19]. Catalysis application of trisodium phosphate is found in glycerol carbonate synthesis, synthesis of β-hydroxyl ketone and methanolysis [18, 20, 21].

As trisodium phosphate provides alkali property, it can be used as the catalyst for transesterification in biodiesel production. Trisodium phosphate can give high yield of biodiesel under mild reaction condition. Therefore, this research used trisodium phosphate to be impregnated on the bottom ash surface. The impregnation helps to disperse active site on the surface of the support and the catalyst might be used several times, reducing the use of active site compound [22, 23]. Trisodium phosphate in this research was provided by Thailand Institute of Nuclear Technology (Public Organization). Trisodium phosphate was obtained as the by-product from the separation process of monazite extraction. It is solid crystal with rod-like shape. In addition, its colour is white and it contains water inside the molecule structure.

In conclusion, this research is interested to combine the use of bottom ash and trisodium phosphate, providing the effective catalyst for transesterification reaction in biodiesel production. It is beneficial that the values of by-products, which are bottom ash and trisodium phosphate, can be extra increased. The results of this research can help to reduce the cost of catalyst used for biodiesel production. This leads to the decrease of biodiesel production cost so that the price of biodiesel is attractive, compared to fossil fuel. Moreover, the increased use of biodiesel can support the energy security in the future as raw materials for biodiesel production are significantly abundant in Thailand.

1.2 Objective of research

1.2.1 To study the effect of the percentage of trisodium phosphate loading, impregnation temperature and calcination temperature on the %FAME.

1.2.2 To study the suitable methanol to oil ratio and test reusability of catalyst.

1.3 **Scope of research**

       1.3.1 To study trisodium phosphate loading at 10, 20, 30 and 40 wt% in wet impregnation method using bottom ash as the supporter.

       1.3.2 To study operating temperature of wet impregnation at room temperature, 40, 60 and 80 °C.

       1.3.3 To study variable conditions in catalyst preparation by using Box-Behnken design.

       1.3.4 To study the calcination temperature at 150, 250, 350 and 450 °C.

       1.3.5 To study the suitable ratio of oil to methanol at 1:9, 1:12, 1:15 and 1:18.

       1.3.6 To study the reusability of the catalyst.

1.4 Benefits of work

       1.4.1 To be able to obtain the suitable conditions for catalyst preparation and understand the effect of each parameter on the %FAME.

       1.4.2 To be able to add more values on bottom ash and trisodium phosphate.

       1.4.3 To be able to provide alternative application of by-products (bottom ash and trisodium phosphate).

1.4.3 To be able to investigate the performance and the reusability of bottom ash impregnated by trisodium phosphate to catalyze transesterification reaction in biodiesel production.

Chapter 2 Literature Review

This chapter presents several related researches which study about bottom ash and trisodium phosphate for their properties and application. Related researches were compiled as the guidelines for implementing this thesis.

2.1 The properties of ash

Chindaprasert et al. (2009) [9] compared the properties between fly ash and bottom ash which are from Coal power plant (Mae Moh, Lampang, Thailand). X-Ray fluorescence was used to verify types and amount of compositions. From the results, fly ash and bottom ash were mostly composed of SiO_2, Al_2O_3, CaO, and Fe_2O_3.

2.2 The catalysis application of ash

Babajide et al. (2010) [24] studied about the use of coal fly ash as a catalyst in biodiesel production. Fly ash was used in base impregnation method to prepare the catalyst. From the results, the highest conversion was 86.13%. The catalyst was prepared from fly ash impregnated with 5 wt% KNO_3. The methanol to oil ratio used in the reaction was 15:1 with stirring rate of 700 rpm at 160 °C for 5 hrs. The reusability was tested. The percentage of conversion decreased from 86.13 to 47.32 and 23.56%, respectively. It indicated that the prepared catalyst was deactivated from the leaching of active site during the reaction.

Bhandari et al. (2015) [25] studied about the transesterification of soybean oil using fly ash-based catalyst. Coal fly ash was treated using hydrochloric acid (10%) at 80 °C for 1.5 h then washed using NaOH at the NaOH/fry ash ratio of 1:1 to 1:2 under the temperature between 400 and 600 °C for 1 hr. After the catalyst preparation, catalysts were used in transesterification reaction of soybean oil. In the

transesterification, biodiesel yield of 81.2% was obtained using 6:1 methanol/oil ratio at 65 °C for 8 h and 3 wt% catalyst.

Inayat et al. (2020) [15] studied about the catalytic air gasification of palm kernel using coal bottom ash as catalyst for parametric analysis and optimization. The interesting parameters are reaction temperatures, catalyst loadings and airflow rates. After the reaction, the most impact parameter on the increase of hydrogen and carbon monoxide was reaction temperature while air flow rate affected the increase of methane and carbon dioxide. Catalyst loading provided higher amount of hydrogen and carbon monoxide but lower amount of methane and carbon dioxide. The best condition in this research was 14.50 wt% of catalyst loading with air flow rate of 2.5 L/min under 850 °C.

Kotwal et al. (2009) [26] studied about transesterification using fly ash-based catalyst. This research varied the amount of KNO_3 loadings and calcination temperatures. Fly ash was impregnated using 3, 5, 10, 15, 20, 35 and 40 wt% KNO_3. The calcination temperature was operated at 773, 873, and 973 K, respectively. Next, catalysts were used for biodiesel catalysis. The highest conversion was 87.5% using catalyst impregnated 5 wt% and calcined at 773 K. However, when increasing KNO_3 loading, oil conversion was dropped since the lower degree of dispersion might be affected, resulting to less catalytic.

Loy et al. (2018) [14] studied about syngas production using rice husk. The pyrolysis of rice husk was catalyzed using bottom ash to compare the catalytic performance with commercial catalysts (nickel and natural zeolite). The compositions of bottom ash were SiO_2, Fe_2O_3, CaO and Al_2O_3, respectively. The catalyst loading to rice husk was 1:10 and then was pyrolyzed. From the results, the bottom ash used as catalyst generated more syngas and less coking than those of commercial catalysts.

Manique et al. (2017) [27] studied about zeolite synthesis using alternative source "coal fly ash". After the hydrothermal process by NaOH, the zeolite in form of

sodalite was produced. The variables of this research were methanol to oil ratios, sodalite loadings and reaction times. The optimal methyl ester content was 95.5% with a 12:1 of methanol to oil molar ratio and 4 wt% sodalite loading. In this study, the reaction time was 120 minutes and the methyl ester yield increased with time.

2.3 The catalysis application of trisodium phosphate

De Filippis et al. (2005) [28] examined the use of trisodium phosphate to catalyze biodiesel reaction. This research used many types of sodium catalyst such as Na_3PO_4, $Na_3PO_4 \cdot 12H_2O$, $Na_5P_3O_{10}$ and NaOH. The methyl ester yields from the use of anhydrous and hydrated trisodium phosphate as catalysts were 82.4 and 65.3 wt%. The catalytic property of both trisodium phosphate types was lower than that of sodium hydroxide. For the comparison between anhydrous and hydrated trisodium phosphate, the methyl ester yield dropped when the system was contaminated by water.

Jiang et al. (2010) [29] chose sodium phosphate for catalysis in biodiesel reaction. The variables of this research were mass ratios of catalyst to oil, molar ratios of methanol to oil, reaction temperatures, rotation speeds and catalyst forms. The rotation speeds had more effect on biodiesel yield than other variables. In this research, biodiesel yield were obtained more than 90% in 2 hours. The catalyst had great activity and can be reused for 8 times with no activity loss because of small dissolution.

Thinnakorn and Tscheikuna (2014) [30] used sodium phosphate as heterogeneous catalyst to catalyze transesterification reaction. The parameters were methanol to oil ratios, operating temperatures, mass ratios of catalyst to oil and the amount of water and free fatty acid in the system. Increasing molar ratio of methanol to oil provided faster rate of reaction, but the rate of reaction was constant when molar ratio of methanol to oil was higher than 18:1. Higher reaction temperature

increased the rate of reaction but reduced the amount of glycerol. Increasing the amount of catalyst tended to increase methyl ester yield. The presence of water and free fatty acid affected the initial stage of reaction, but in the equilibrium the yield of methyl ester was the same.

Yatish et al. (2016) [31] studied about the synthesis of methyl ester from Garcinia gummi-gutta, Terminalia belerica and Aegle marmelos seed oil via transesterification reaction using sodium phosphate as the catalyst, and investigated the characterization of fuel properties. The reaction was carried out with stirrer speed at 700 rpm and reaction temperature of 70 °C. The methyl ester yield depended on the fatty compound in the oil. The fuel properties of synthesized biodiesel were standardized using ASTM D-6751 standard.

Suksuchot (2018) [32] studied about the recrystallization of trisodium phosphate and the experimental design using Box Behnken method. The variables of this research were methanol to oil ratios, catalyst loadings and reaction times. The suitable conditions for the reaction were at 60 °C of reaction temperature, 600 rpm of stirrer speed, 14.91:1 of methanol to oil ratio, 5.54 wt% of catalyst loading and 153.89 minutes of reaction time.

Chapter 3 Theory

This chapter presents the principal knowledge of biodiesel, coal ash, trisodium phosphate and wet impregnation method.

3.1 Biodiesel

Biodiesel is an alternative energy which can be produced from vegetable oil, animal fat, waste cooking oil or seaweed oil. These oils react with methanol or ethanol using the catalyst to convert triglyceride into methyl ester or ethyl ester and glycerol. The properties of these ester compounds, called 'biodiesel', are similar to fossil diesel. Therefore, biodiesel can be used in diesel engine [4].

The use or synthesis of biodiesel have many methods as follows.

3.1.1 Direct use of vegetable oil

Rudolf Diesel who invented the first diesel engine directly used peanut oil in diesel engine. At the present, vegetable oil can still be used in agricultural engine equipped with heater to reduce the oil viscosity before entering the combustion chamber [33].

3.1.2 Biodiesel blended with diesel

As some properties of biodiesel are not suitable to be directly used in diesel engine, some amount of biodiesel was blended with fossil diesel using suitable solvent. This can reduce the use of fossil diesel and also prevent some problems caused from pure biodiesel. Biodiesel blended with fossil diesel was used and known in Thailand as Biodiesel B5 [33].

3.1.3 Microemulsion

Microemulsion is a method which help to prevent some problems from high viscosity of vegetable oil. This method reduces the viscosity of vegetable oil by transforming vegetable oil into colloid form. Then, it is mixed with methanol, ethanol or 1-butanol. The biodiesel produced from this method showed similar properties of diesel. However, when it was tested, the carbon buildup was found around the nozzle and valve in the engine [34].

3.1.4 Pyrolysis

Pyrolysis process is used to convert a compound using heat and catalyst. The temperature used in this method is very high around 450 to 600 ℃. The compound molecules were broken into smaller ones after the process. It is difficult to control this process pathway because of the diversity of reaction [34].

3.1.5 Transesterification

Transesterification is the reaction between triglyceride and alcohol using the catalyst to convert these compounds into ester compound and glycerol as shown in Figure 3.1. This reaction contains 3 steps. The first step, triglyceride is converted into diglyceride. Next, diglyceride is converted into monoglyceride. Finally, monoglyceride is converted into glycerol. Each step will produce one ester compound [35].

$$CH_2 - O - C - R_1 \overset{O}{\overset{\|}{}}$$

$$CH - O - C - R_2 \overset{O}{\overset{\|}{}} \quad + \quad 3CH_3OH \longrightarrow \quad CH_3 - O - C - R_2 \overset{O}{\overset{\|}{}} \quad + \quad CH - OH$$

Triglyceride   Methanol   Mixture of fatty esters   Glycerin
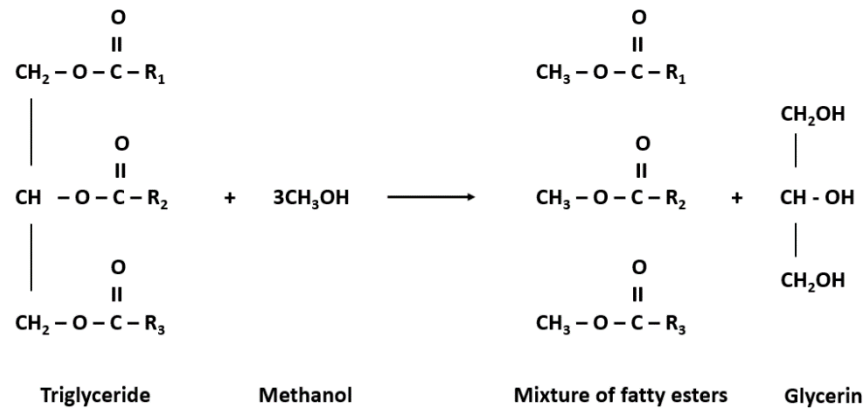
Figure 1 *Transesterification reaction*

From the Figure 1, it showed that the transesterification reaction is reversible. The excess alcohol used can control the reaction to produce the product. The catalysts in this reaction have 3 types, such as acid catalyst, base catalyst and enzyme [36].

3.1.6 Esterification

Esterification is the reaction of which free fatty acid react with alcohol using acid catalyst as shown in Figure 2.

$$R - COOH \quad + \quad R' - OH \longrightarrow R - COOR' \quad + \quad H_2O$$

Fatty acid   Alcohol   Biodiesel
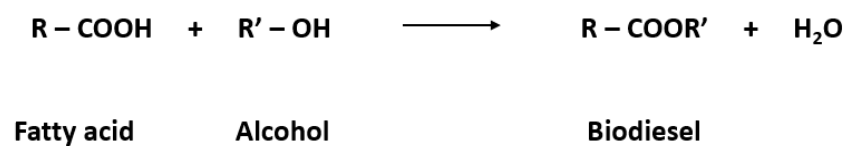
Figure 2 *Esterification reaction*

3.2 Bottom ash

The bottom ash is generated from coal combustion in coal power plant. Bottom ash is a material which has high porosity, and can keep a lot of water which is suitable for the use in internal curing material of concrete [37]. One of application of bottom ash is the use of bottom ash for making interlocking block [38]. In 2017, coal bottom ash had been considered to use as alternative for construction material, material for wastewater treatment, structural filling and soil improvement [39].

The composition of bottom ash was similar to fly ash such as SiO_2, Al_2O_3, CaO and Fe_2O_3. Table 1 showed the composition of coal fry ash and bottom ash. From these compositions, there are several applications from the use of bottom ash.

Table 1 *Chemical compositions of fly ash and bottom ash*

| Composition	Mae Moh coal power plant [9]		BLCP power plant [42, 43]		Coal fired power plant Federico II [44]	
	Fly ash	Bottom ash	Fly ash	Bottom ash	Fly ash	Bottom ash
SiO_2	38.7	38.8	61.09	63.18	46.2	42.72
Al_2O_3	20.8	21.3	20.35	19.48	27	24.33
FeO_3	15.3	12.1	-	-	-	-
CaO	16.6	16.5	2.32	2.05	9.07	15.14
Na_2O	1.3	1	0.79	1.05	-	-
TiO_2	0.5	0.8	-	-	2.6	3.02
MgO	1.3	1.7	1.35	1.28	-	-
K_2O	2.1	2.5	1.36	1.10	1.41	2.24
SO_3	2.6	2.4	0.28	0.12	-	-
LOI	0.8	2.9	5.68	2.80	-	-
Cr_2O_3	-	-	-	-	0.03	0.09
Fe_2O_3	-	-	5.20	7.32	10.61	10.64
NiO	-	-	-	-	0.01	0.03
MnO	-	-	-	-	0.11	0.01
SrO	-	-	-	-	0.41	0.7

From the chemical compositions of bottom ash, it was used as the catalyst or support of catalyst. The use of bottom ash as the catalyst was found in biomass gasification reaction, air gasification of palm kernel, steam gasification of palm oil waste and pyrolysis of rice husk to produce syngas [14, 15, 40, 41].

3.3 Trisodium phosphate

Trisodium phosphate is an inorganic compound which consists with 3 sodium atoms and phosphate group in crystal structure. The properties of trisodium phosphate can be seen in Table 2. Trisodium phosphate was used as a laxative, dietary supplement and for electrolyte replacement purposes [19]. The uses of trisodium phosphate as the catalyst were found in many reactions such as transesterification, glycerol carbonate synthesis, and Knoevenagel reaction [18, 30, 45].

The source of trisodium phosphate in this thesis is from Thailand Institute of Nuclear Technology (Public Organization). Trisodium phosphate is the by-product from the monazite ore extraction using alkali process as shown in Figure 3.

Table 2 Trisodium phosphate properties [17].

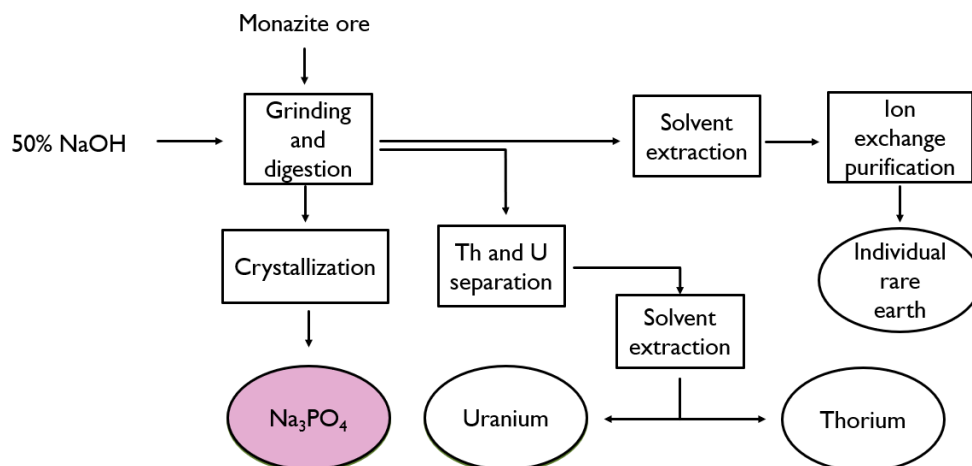| Properties	Description
Melting point	1340 °C
Density	2.536 g/cm^3 (Temp: 17.5 °C)
Form	Powder
Color	White
Water solubility	Soluble in water. Insoluble in ethanol and carbon disulfide

Figure 3 *The extraction monazite ore using alkali process diagram [32]*

3.4 Wet impregnation method

Impregnation is the one of favorite techniques to prepare the catalyst. This technique uses the mixing of non-homogeneous substances. The catalyst precursor is mixed with the support of catalyst. The active sites (in liquid phase) are dispersed on the support or other active sites in solid phase [46].

The impregnation method has two types, based on the volume of solution. For wet impregnation, the use of solution is excess. After wet impregnation, the catalyst is dried to remove excess solvent. For dry impregnation, the volume of solution is fixed or slightly less than the pore volume of support [22].

Some factors in impregnation method can affect the properties of catalyst such as temperature of impregnation. The impregnation temperature influence the solubility of precursor (maximum loading) or solution viscosity [22] which can modify the properties of catalyst.

The advantage of impregnation method is inexpensive. It is also easy to prepare active layer on catalyst surface and control the configuration [22].

3.5 Box-Behnken experimental design

This method apply statistic knowledge to design the experiment for multivariate [47] which help to find the impact of variable factors in the experiment. The design of experiment can decrease the number of the experimental batches as some batches are not needed to be carried out, leading to lower expenditure. The experimental design from Box-Behnken can study the impact and interaction of variable factors using Box-Behnken form. This method has good efficiency and it is often used to design the experiment.

The experiment from Box-Behnken distribute the values of the variable into 3 levels as low, middle and high. The created equation for predicting the response is suitable for quantitative factors such as molar ratio, temperature, pressure and time [32].

The design of experiment has a number of experiments as $N=2k(k-1)+C_0$, where k is number of factors and C_0 is the number of central points. Box-Behnken design was used in several applications such as optimization of the spectroanalytical method, optimization of chromatographic methods, optimization of capillary electrophoresis, optimization of electroanalytical methods and optimization of sorption process [47].

In example, Dwivedi and Sharma (2015) studied the application of Box-Behnken design in optimization of biodiesel yield. In this research, the variable conditions were methanol/oil ratios, reaction times, reaction temperatures and catalyst amounts as shown in Table 3 [48].

Table 3 *Independent variables used for Box-Behnken in transesterification*

Variables	Symbols	Level		
		-1	0	1
Methanol/oil ratio	A	3	7.5	12
Reaction time	B	30	75	120
Reaction temperature	C	35	55	75
Catalyst amount	D	0.30	0.90	1.5

The regression and graphical of the data were analyzed by The Design Expert 8.0.6 software. The maximum yield was obtained by the response of the design experiment for biodiesel production. The results of the experiment were shown in Table 4 and the regression for the estimation of predicted value was given as follow:

Yield $= 70.58 + 7.96 \times A - 2.40 \times B - 4.31 \times C + 9.58 \times D + 12.25 \times A \times B - 14.74 \times A \times C + 24.95 \times A \times D - 2.12 \times B \times C + 8.63 \times B \times D - 0.71 \times C \times D - 4.08 \times A^2 - 20.34 \times B^2 - 9.80 \times C^2 - 0.88 \times D^2$.

From the optimization of transesterification, 98.4% of biodiesel yield was found with methanol/oil ratio is 11.06:1 using 1.43 w/w% of KOH for 81.4 minutes at 56.6 ℃. All variables had significantly effects on biodiesel yield [48].

Table 4 *Responses for transesterification of pongamia oil [48]*

Run	A	B	C	D	Pongamia biodiesel yield (%)	
					Experiment response	Predicted response
1	3	75	35	0.9	54.05	38.30121
2	7.5	30	75	0.9	30.7	40.65419
3	7.5	120	35	0.9	34.3	44.46662
4	12	30	55	0.9	45.8	44.26767
5	3	75	55	0.3	66.6	73.0205
6	7.5	75	75	1.5	69.6	64.45295
7	7.5	120	75	0.9	27.9	31.59908
8	12	75	75	0.9	40.5	45.60841
9	7.5	75	35	1.5	70.8	74.4905
10	7.5	30	35	0.9	28.6	45.02173
11	3	30	55	0.9	54.6	52.843
12	7.5	120	55	1.5	74.8	65.15453
13	7.5	75	55	0.9	79.4	70.57813
14	7.5	30	55	1.5	74.8	52.70988
15	7.5	75	75	0.3	59.9	46.71673
16	7.5	75	55	0.9	74.6	70.57813
17	7.5	120	55	0.3	17.3	28.74854
18	3	75	55	1.5	22.8	442.27674
19	7.5	75	35	0.3	58.26	53.91427
20	7.5	75	55	0.9	79.5	70.57813
21	3	120	55	0.9	31.5	23.53782
22	7.5	30	55	0.3	51.8	50.80341
23	3	75	75	0.9	59.6	59.15867
24	7.5	75	55	0.9	32.8	70.57813
25	12	75	55	1.5	94.4	108.1015
26	7.5	75	55	0.9	86.6	70.57813
27	12	75	35	0.9	93.9	83.70095
28	12	120	55	0.9	71.7	63.96264
29	12	75	55	0.3	38.4	39.04525

Chapter 4 Methodology

This chapter mentions about methodology. It gives the details about raw materials, chemicals, experimental procedure, instrumental analysis, catalyst characterization etc. which were used in this research to study the effect of percentage of impregnation, impregnation temperatures and calcination temperatures on the bottom ash impregnated using trisodium phosphate.

4.1 Raw Materials and Chemicals

4.1.1 Bottom ash, obtained from Thailand Institute of Nuclear Technology (Public Organization). The bottom ash was from Coal Power Plant (BLCP), located in Mabtaphut, Rayong.

4.1.2 Trisodium phosphate (Na_3PO_4), obtained from Thailand Institute of Nuclear Technology (Public Organization). Trisodium phosphate is the by-product from separation process of monazite ore extraction using alkali [32].

4.1.3 Methanol (CH_3OH), (> 99.5%), AR grade from Quality Reagent Chemical Co., Ltd.

4.1.4 Palm olein oil, 'Morakot' brand, purchased from a market.

4.1.5 Helium gas (He), 99.99% purity, purchased from Alternative chemical Co., Ltd.

4.1.6 Carbon dioxide gas (CO_2), 99.8% purity, purchased from Linde Co., Ltd.

4.1.7 Nitrogen gas (N_2), 99.99% purchased from Alternative chemical Co., Ltd.

4.1.8 Methyl heptadecanoate ($CH_3(CH_2)_{15}COOCH_3$), analytic grade, purchased from Sigma-Aldrich Thailand Co., Ltd.

4.1.9 Heptane (C_7H_{16}), 99.9% purity, purchased from Quality Reagent Chemical Co., Ltd.

4.2 Equipments

4.2.1 Beakers (100, 250, 600 and 1,000 mL)

4.2.2 Measure cylinder (100 mL)

4.2.3 Magnetic bar (2.5-4 cm in length)
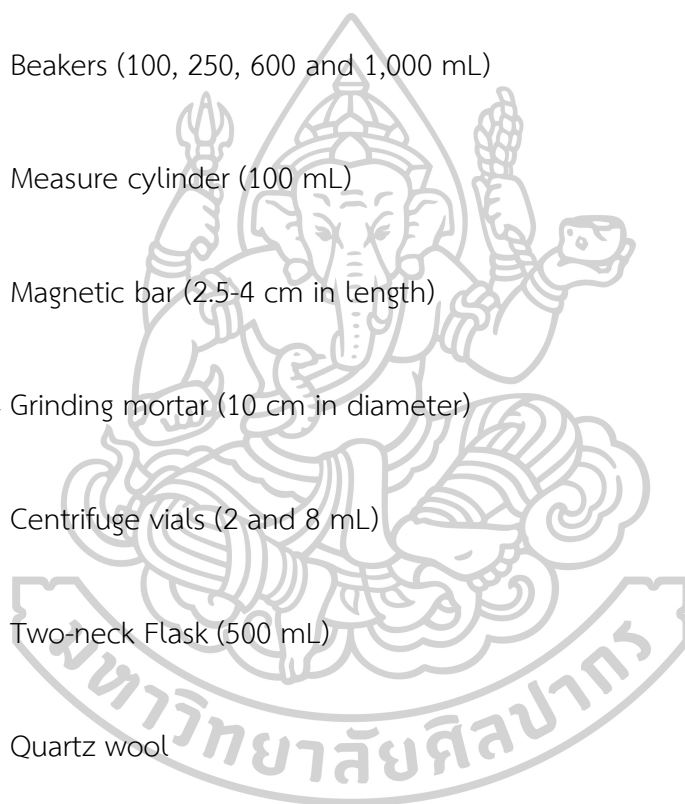
4.2.4 Grinding mortar (10 cm in diameter)

4.2.5 Centrifuge vials (2 and 8 mL)

4.2.6 Two-neck Flask (500 mL)

4.2.7 Quartz wool

4.2.8 Syringe (10 μL)

4.2.9 Ceramic boats

4.3 Experimental Apparatus and Analytical Instruments

4.3.1 Hotplate and magnetic stirrer (CMAGHS7 model, IKA Company)

4.3.2 Incubator (FED 240 model)

4.3.3 Centrifuge (XC 80-2 model, Science city Co., Ltd.)

4.3.4 Laboratory chamber furnace (from Chavachote furnace)

4.3.5 BET (Brunauer-Emmett-Teller) (BELSORP-mini II Microtrac model, BEL Company)

4.3.6 XRD (X-ray diffraction) (model D8 Advance, Bruker)

4.3.7 SEM (Scanning electron microscope) (MIRA3 model, TESCAN Company)

4.3.8 TPD (Temperature program desorption) (Autochem 2910 model, Micromeritics)

4.3.9 Gas Chromatography (GC) (HP 5890 series II model)

4.4 Catalyst Preparation

4.4.1 Trisodium phosphate and bottom ash treatment

Trisodium phosphate and bottom ash used as raw materials need to be treated before the catalyst preparation process. Trisodium phosphate was calcined at 350 °C using the temperature ramp rate of 10 °C/min for 30 minutes to remove water inside

the crystal. The treated trisodium phosphate is then kept in the desiccator to prevent the moisture from the air before use.

For bottom ash, the 100 µm screen tray was used for size selection of bottom ash. Then, 9 g screened bottom ash was added into 50 mL DI water with stirring rate at 500 rpm using 5 cm magnetic bar for 1 hour. The Fe contained in bottom ash was attached on magnetic bar. After removing magnetic bar, the bottom ash was baked at 120 ℃ for 12 hours. Next, 9 g dried bottom ash was treated with 150 mL of 3 M HCl for 60 minutes at 70 ℃ to remove the residue Fe in bottom ash [49]. Finally, treated bottom ash was washed using DI water and was filtered using filter paper No.1 (Whatman) under the help of vacuum pump. Then, bottom ash was baked at 110 ℃ for 3 hours. Finally, residual bottom ash was calcined at 800 ℃ for 2 hours to removed unburnt carbon [50].

It was noted that both raw materials are treated as mentioned above before they are used in the next step. Otherwise, some additional details will be mentioned later.

4.4.2 The effect of the percentage of trisodium phosphate impregnated on bottom ash

The 4% (w/v) trisodium phosphate solution was prepared. Trisodium phosphate of 4 g was dissolved in DI water in 100 mL volumetric flask until the final solution volume was adjusted to 100 mL. The volumetric flash was shaken until trisodium phosphate was well dissolved in DI water. Then, the impregnation of trisodium phosphate on bottom ash was carried out. 100 mL of trisodium phosphate was mixed with 6 g bottom ash with stirring rate of 350 rpm using 2.5 cm magnetic bar on the hot plate. The impregnation temperature was controlled at 60 ℃ for 12 hours. Next, trisodium phosphate-impregnated into bottom ash was dried in an oven at 110 ℃ for 12 hours. After that, dried trisodium phosphate-impregnated into bottom ash

was calcined at 350 °C for 30 minutes using the temperature ramp rate of 10 °C/min. It is noted that this prepared catalyst was labelled as 40% (w/w) impregnation of trisodium phosphate into bottom ash. The impregnation method was modified from the work of Hadiyanto et al. (2016) [51].

This procedure mentioned above was repeated using 3, 2, and 1% trisodium phosphate solution in order to prepare 30, 20 and 10% impregnation, respectively. All prepared catalysts were used as the catalyst for biodiesel production.

4.4.3 The effect of impregnation temperatures

The catalyst preparation was carried out using the same procedure mentioned in 4.4.2. However, the suitable percentage of trisodium phosphate impregnation was chosen from the results in 4.4.2. In addition, the temperature impregnation was performed at 40, 50 and 70 °C, respectively. Next, the prepared catalysts were used as the catalyst for biodiesel production.

4.4.4 The effect of calcination temperatures

The catalyst preparation was carried out using the same procedure mentioned in 4.4.2. However, the suitable percentage of trisodium phosphate impregnation and suitable impregnation temperature were chosen from the results in 4.4.2 and 4.4.3. In addition, the calcination temperature was operated at 150, 250 and 450 °C, respectively. Next, the prepared catalysts were used as the catalyst for biodiesel production.

4.4.5 The study of variable designed experiment using Box-Behnken

The variables in this research are the percentage of trisodium phosphate loadings, impregnation temperatures and calcination temperatures. Box-Behnken

method distributed value of these variables into 3 levels as low, middle and high as shown in Table 5.

Table 5 *Factors and levels of catalyst preparation for biodiesel production.*

Factor	Symbol	Level		
		-1	0	1
The percentage of trisodium phosphate loading	A	20	30	40
Impregnation temperature (°C)	B	40	60	80
Calcination temperature (°C)	C	250	350	450

The catalysts were prepared as followed in Table 6. All of experimental designs using Box-Behnken were carried out for catalysis in biodiesel production. Then, the calculation was performed for the impact and interaction of variables.

Table 6 *The experimental design using Box-Behnken*

Experiment	Factor		
	A (% trisodium phosphate loading)	B (Impregnation temperature, °C)	C (Calcination temperature, °C)
1	-1 (20)	-1 (40)	0 (350)
2	1 (40)	-1 (40)	0 (350)
3	1 (40)	1 (80)	0 (350)
4	1 (40)	0 (60)	-1 (250)
5	-1 (20)	0 (60)	-1 (250)
6	0 (30)	-1 (40)	-1 (250)
7	-1 (20)	0 (60)	1 (450)
8	0 (30)	0 (60)	0 (350)
9	1 (40)	0 (60)	1 (450)
10	0 (30)	-1 (40)	1 (450)
11	0 (30)	0 (60)	0 (350)
12	0 (30)	1 (80)	1 (450)
13	0 (30)	0 (60)	0 (350)
14	-1 (20)	1 (80)	0 (350)
15	0 (30)	1 (80)	-1 (250)

4.5 Biodiesel Production

4.5.1 The effect of the ratios of oil to methanol

The biodiesel production was carried out following the work of Suksuchot (2561) [32]. The palm oil of 113 mL (the ratio of oil to methanol is 1:15) were added into a 2-neck flask and then 5 g prepared catalyst was added into palm oil with stirring rate of 600 rpm using 4 cm magnetic bar. The mixture was heated to 60 °C and was controlled at this temperature, using a hot plate. After the mixture temperature reached to 60 °C, 71.5 mL methanol was then added into 2-neck flask. The loss prevention of methanol in the reaction was performed using condensing unit connected to the top of the 2-neck flask. The cold water at 4 °C was used as the cooling media in condensing unit with the flow rate of 20 L/min. The operating unit for biodiesel production can be seen in the Figure 4.

The experiments were repeated using the several ratios of oil to methanol which are 1:9, 1:12 and 1:18 to find the suitable ratio between methanol and oil which provides the highest %FAME. This experiment will be repeated after the catalysts which can produce the highest %FAME are obtained in this research.

After 3 hours of reaction, the products, reactants, and catalysts in the flask were separated using the centrifuge at the rotation speed of 3,000 rpm for 45 minutes. The top part in the centrifugal tube was assigned to methyl ester (or biodiesel) and the lower part was glycerol. The rests, which were located in the lowest layer under the glycerol, were residual methanol, palm oil and catalysts, respectively. The methyl ester was added into a beaker and then was baked in an oven at 110 °C for 12 hours to remove residual methanol. Then, the content of methyl ester was tested using GC technique.

Figure 4 *Biodiesel production unit*

4.5.2 The study in the reusability of the catalyst

The reusability of the catalyst can be carried out using the same procedure mentioned in 4.5.1. The prepared catalyst was chosen using the suitable conditions of catalyst preparation from 4.4. After the reaction, the catalyst was separated using a centrifuge. Then, the catalyst was washed using 99.5% methanol of 20 mL for several time [18, 52]. Next, the catalyst was baked in an oven at 110 °C overnight. The rest catalyst was then used for biodiesel production with the same amount ratio of palm oil and methanol. The rest catalyst from each batch of biodiesel production will be used several times until the percentage of methyl ester is dropped [53, 54].

4.6 Catalyst Characterization

4.6.1 Brunauer-Emmett-Teller (BET)

BET technique is used to analyze surface area, volume and pore size of the catalyst. These values were obtained using N_2 physisorption. First of all, the catalyst was pretreated using 50 mL/min of Helium gas at 180 °C for 3 hours. Then, the sample cell was equipped in BET equipment. Liquid nitrogen was added into lifting part. The samples were cooled to -196 °C. The nitrogen was fed into sample cell, then the volume of N_2 and pressure were measured. Nitrogen was adsorbed onto the catalyst surface. After the catalyst cannot adsorb more nitrogen, the desorption of nitrogen on the catalyst surface began. Therefore, BET characterization was completed. The BET instrument can be seen in Figure 5.

The preparation of BET characterization is as follow;

1. The catalyst was baked in an oven at 110 °C for 24 hours.

2. 0.1 g catalyst was added into the sample cell for BET characterization.

3. Catalyst was pretreated at 180 °C for 3 hours.

4. Surface area, pore volume, and pore size of catalyst were analyzed using BET.

Figure 5 *BET (Brunauer-Emmett-Teller) instrument (BELSORP-mini II Microtrac model, BEL Company)*

4.6.2 X-ray diffraction (XRD)

The XRD technique was used to obtain the crystal structure, alignment of atom and crystalline size of the catalyst, using the pattern of diffraction and scattering of X-ray. The uniqueness of diffraction can define the composition of the catalyst. The diffraction of X-ray in crystal relies on Bragg's law. In this work, XRD is used to define the presence of trisodium phosphate and the composition of bottom ash. The XRD instrument was shown in Figure 6.

Figure 6 *XRD (X-ray diffraction) model D8 Advance, Bruker*

4.6.3 Scanning electron microscopy (SEM)

Scanning electron microscopy is an instrument for studying the morphology of materials. In addition, EDS technique (Energy Dispersive Spectrometry) coupled with SEM can be used to analyze the composition of materials. The image captured using SEM shows 2-dimension picture with more than 200,000 times magnification. The electron gun in SEM produces the electron moving with high velocity through condenser lens and transforming into electron beam. The material surface was shined by electron beam and then the secondary electron from the material surface come out of the surface. The secondary electrons are detected by a detector. This signal is transformed into visual image of the surface. The SEM instrument can be shown in Figure 7.

The preparation for SEM characterization is as follow;

1. The samples were attached onto an adhesive sheet and then the sheet was attached onto steel stick.

2. The sample which is nonmetal have to be coated with gold layer to clarify the surface and prevent sparking from the electron deposition. The coating process takes about 40 minutes.

3. Steel stick was attached into the sample holder in the SEM instrument for the measurement.

Figure 7 *SEM (Scanning electron diffraction) instrument (NIRA3 model, TESCAN Company)*

4.6.4 Temperature programmed desorption (TPD)

Temperature programmed desorption technique is used to obtain the desorption pattern between absorbent (gas) and absorbate (catalyst) used in the test. If acid site of catalyst is measured, the absorbent will be basic gas such as ammonia. This is called NH_3-TPD. In contrast, the acidic gas such as carbon dioxide is used to determine basic site, known as CO_2-TPD. The area under the graph plotted between intensity and temperature indicates the amount of active site. The temperature at desorption peak showed the intensity of acid or base site of the catalyst. The TPD instrument can be seen in Figure 8.

The preparation for CO_2-TPD characterization is as follow;

1. 0.1 g catalyst was added into quartz wool. Then quartz wool was placed into U-tube.

2. U-tube was then equipped into TPD instrument.

3. The catalyst in U-tube was heated to 150 °C and held for 1 hour to remove water in catalyst. Then, the catalyst was cooled down to 50 °C.

4. CO_2 was fed into U-tube for adsorption. Then, the desorption began by increasing the temperature to 800 °C and holding at this temperature for 1 hour.

5. After the analysis, the graph was used for basic site calculation.

Figure 8 *TPD (Temperature Programmed Desorption) instrument (Autpchem 2910 model, Micromeritics)*

4.6.5 Gas chromatography flame ionization detector (GC-FID)

GC technique is used to separate the composition of the mixture using the different movements of each composition on the stationary phase under the convection of mobile phase. For flame ionization detector, the sample was ionized using the flame and then the carrier gas took the ionized sample to the detector. GC-FID instrument is presented in Figure 9.

The preparation of sample for GC analysis is as follow;

1. 10 mg/mL methyl heptadecanoate was prepared using 1 g of methyl heptadecanoate dissolved in heptane until the final solution was 100 mL.

2. 0.05 g biodiesel from the reaction was added into a vial.

3. 1 mL of heptadecanoate (10 mg/mL) was added into the biodiesel. The vial was shaken until the mixture was well mixed.

4. The prepared sample was taken into GC-FID. The instrument uses Helium gas as carrier. The temperatures of the injector, oven and detector were controlled at 200, 180 and 230 °C, respectively.

5. The temperature of oven was increased to 220 °C.

6. After analysis, the graph can show the position and area of compositions. This can be used to calculate the amount of composition.

Figure 9 *GC-FID (Gas Chromatography-Flame ionization) instrument (HP 5890 series II model)*

4.6.6 X-ray fluorescence (XRF)

XRF is analytical method to find the composition of materials. After an element in the sample was radiated with X-ray light, the element will emit fluorescence X-ray radiation with discrete energies which are characteristic in each element [55]. The XRF instrument is presented in Figure 10.

The sample preparation was described below.

1. The catalyst is in the form of powder. Thus, the film was used to support the catalyst powder.

2. The film was stretched covering the one end of the holder, as seen in Figure 11. Then, the powder was added into the holder on the film.

3. The powder was equally levelled before another one end of the holder was closed by a lid.

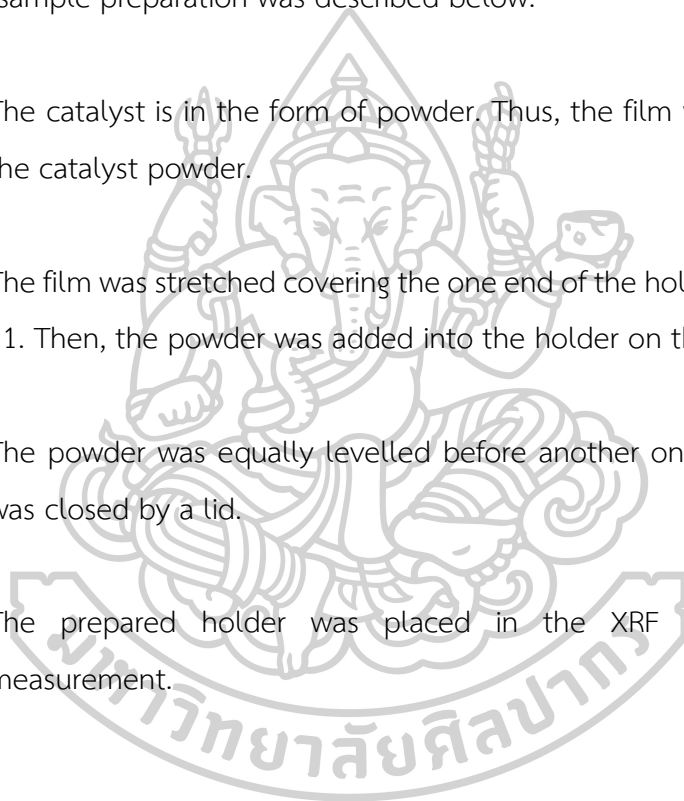4. The prepared holder was placed in the XRF instrument for the measurement.

Figure 10 *XRF (X-ray fluorescence) model S8 TIGER, Bruker*

Figure 11 *Sample holder for XRF instrument*

Chapter 5 Results and Discussions

This chapter shows the results of catalyst characterization and discuss about the effect of trisodium phosphate loadings, impregnation temperatures, calcination temperatures, and methanol to oil ratios on transesterification reaction. Moreover, the Box-Behnken experimental design and reusability of catalyst were also presented in this chapter.

5.1 Bottom ash and trisodium phosphate characterization

5.1.1 XRD

The XRD pattern in Figure 12 shows the peak of ACBT (bottom ash treated with HCl, then calcined at 800 °C for 2 hours) which was mainly consisted with quartz and mullite form, followed by JCPDS no. 83-0539 and 79-1454 databases. It implied that the main composition of ACBT was SiO_2. In Figure 13, it showed the XRD pattern of trisodium phosphate (TSP) from monazite ore extraction process. The peaks in Figure 13 presented the similar pattern followed by JCPDS no. 76-2182 which were assigned to sodium phosphate hydrate.

Figure 14 presented the XRD pattern of 40TSP/ACBT. The peaks in Figure 14 were mainly observed as the peaks of quartz, mullite, and trisodium phosphate (TSP). This might be the well dispersion of trisodium phosphate on the surface of bottom ash. In addition, impregnation of trisodium phosphate might be located with several forms of sodium and phosphate. Therefore, the observation of trisodium phosphate in 40TSP/ACBT catalyst using XRD pattern was unclear.
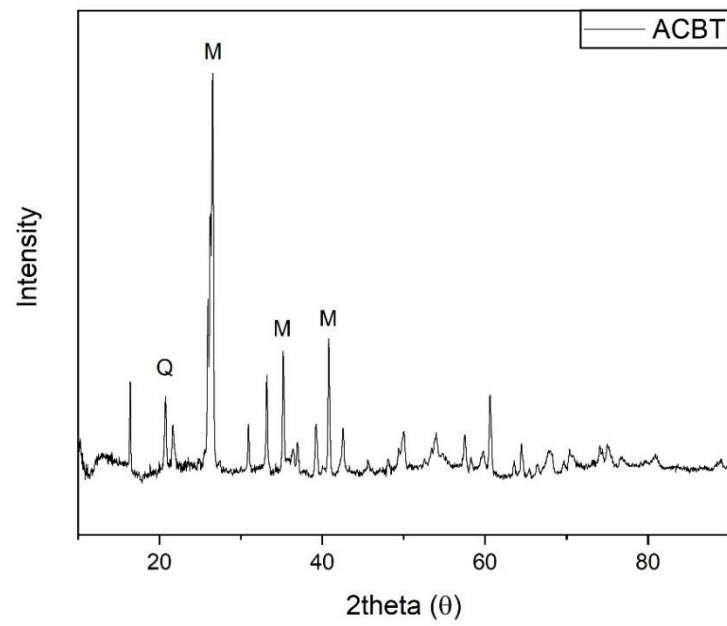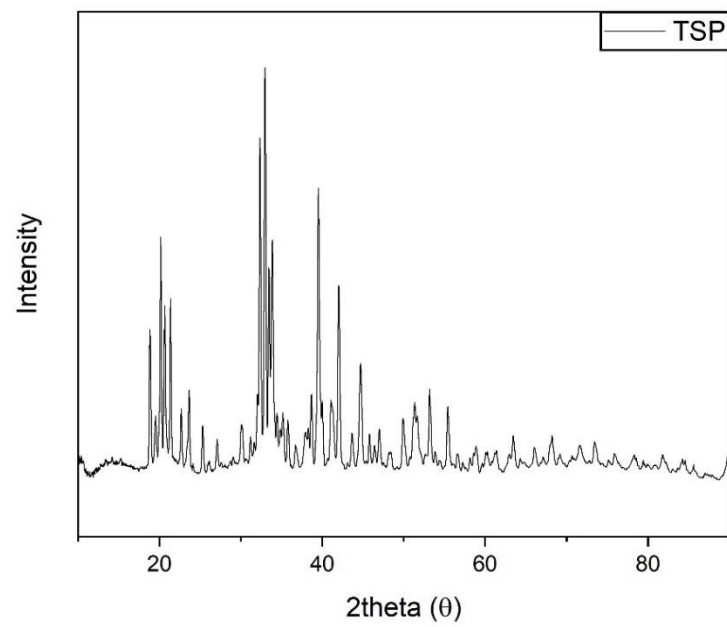
Figure 12 *The XRD pattern of bottom ash*

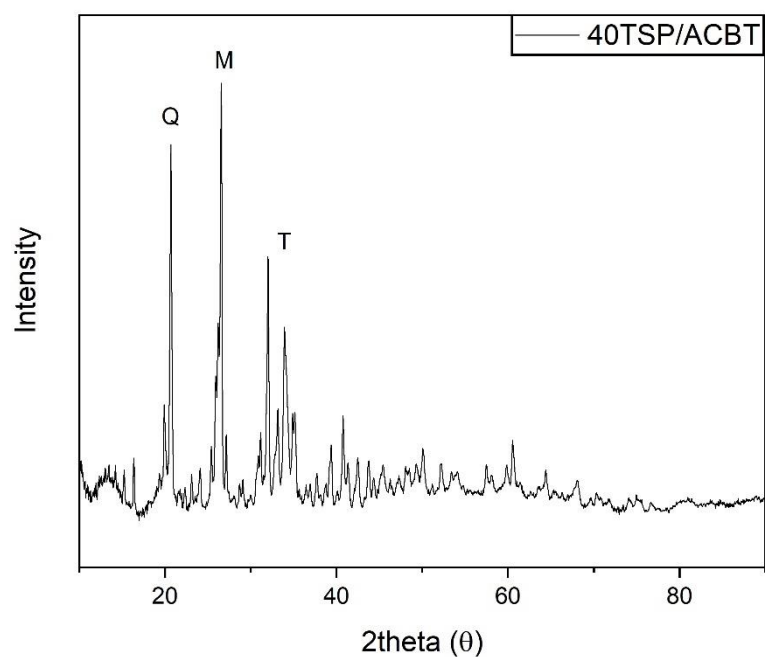**Figure 13** *The XRD pattern of Trisodium phosphate*

Figure 14 *The XRD pattern of 40TSP/ACBT*

The composition of bottom ash was analyzed using X-ray fluorescence instrument as showed in Table 7.

Table 7 *The composition of bottom ash*

Composition of Bottom ash	wt%
SiO_2	64.03
Al_2O_3	20.48
Fe_2O_3	7.30
CaO	3.09
TiO_2	1.98
K_2O	1.83
MgO	0.52
Others	0.55

Trisodium phosphate from monazite ore extraction process was not pure as same as commercial grade. The XRF analysis showed the compositions of trisodium phosphate as seen in Table 8. The main composition of trisodium phosphate was Na and P (>97% in total).

Table 8 *The composition of trisodium phosphate*
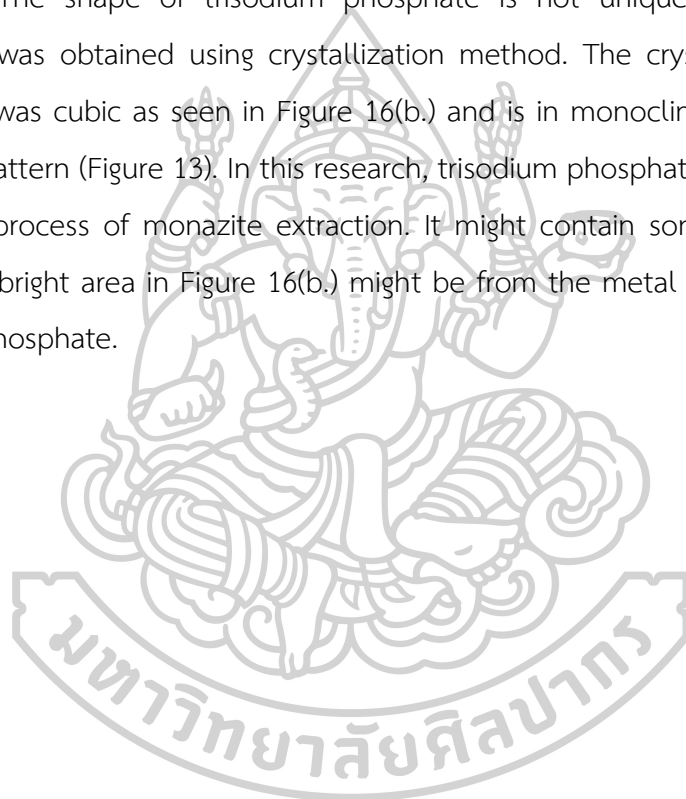
Composition of trisodium phosphate	wt%
Na	53.5
P	43.94
Others	2.56

After the impregnation, 40TSP/ACBT was obtained. The composition of 40TSP/ACBT was showed in Table 9. It was observed that 40TSP/ACBT consisted of high content of Na and P as trisodium phosphate was impregnated on bottom ash using 40 wt% of catalyst.

Table 9 *The composition of 40TSP/ACBT*

| Composition of 40TSP/ACBT	wt%
Si	31.55
Na	21.44
P	19.55
Al	11.33
Fe	7.92
Others	8.20

5.1.2 SEM

The morphology of bottom ash in contrast mode can be seen in Figure 15, using SEM measurement. The appearance of bottom ash looks like condensed solid as bottom ash was melted at high temperature. On the surface of bottom ash, it implied that the porosity was likely low and also some crystal growths were observed outside the surface. For trisodium phosphate, its morphology can be presented in Figure 16. The shape of trisodium phosphate is not unique because trisodium phosphate was obtained using crystallization method. The crystalline of trisodium phosphate was cubic as seen in Figure 16(b.) and is in monoclinic form as observed from XRD pattern (Figure 13). In this research, trisodium phosphate is by-product from separation process of monazite extraction. It might contain some impurity such as metal. The bright area in Figure 16(b.) might be from the metal which contaminated trisodium phosphate.
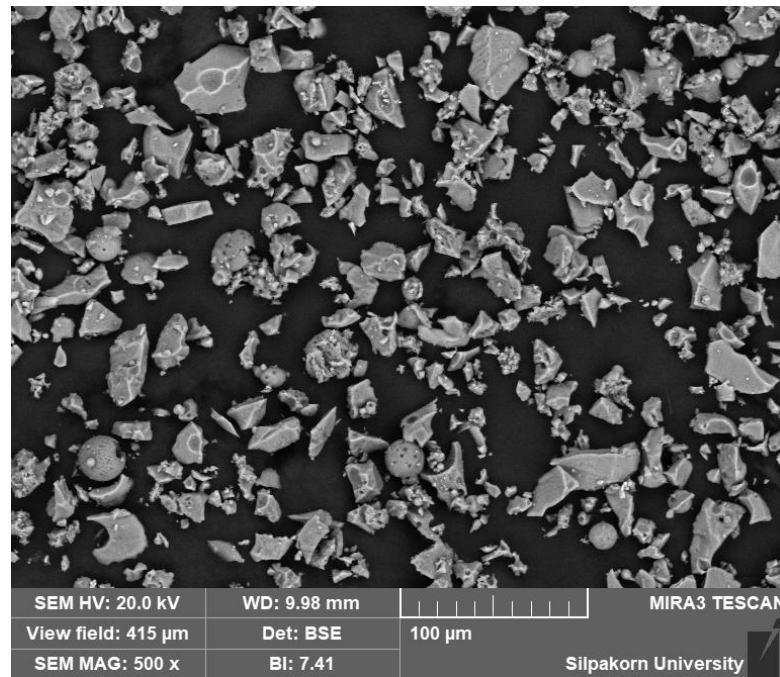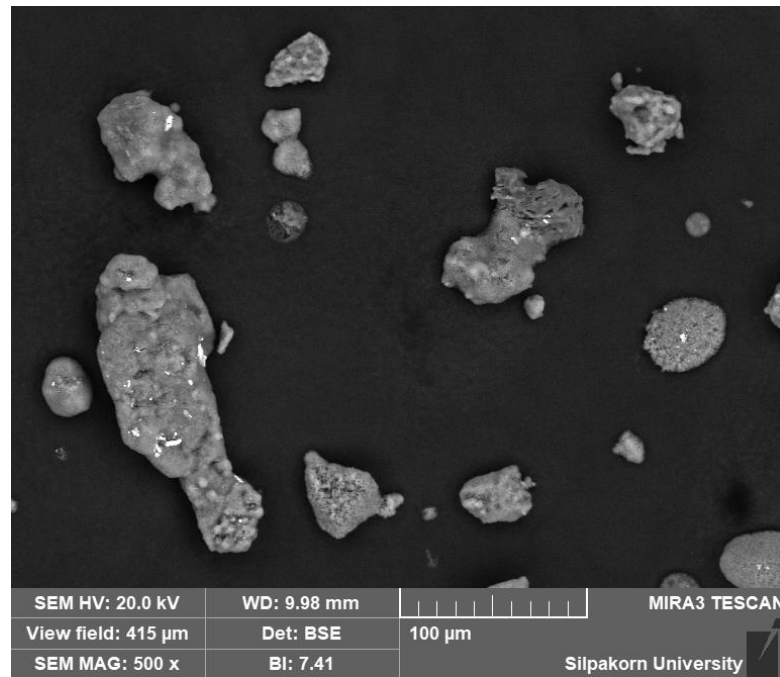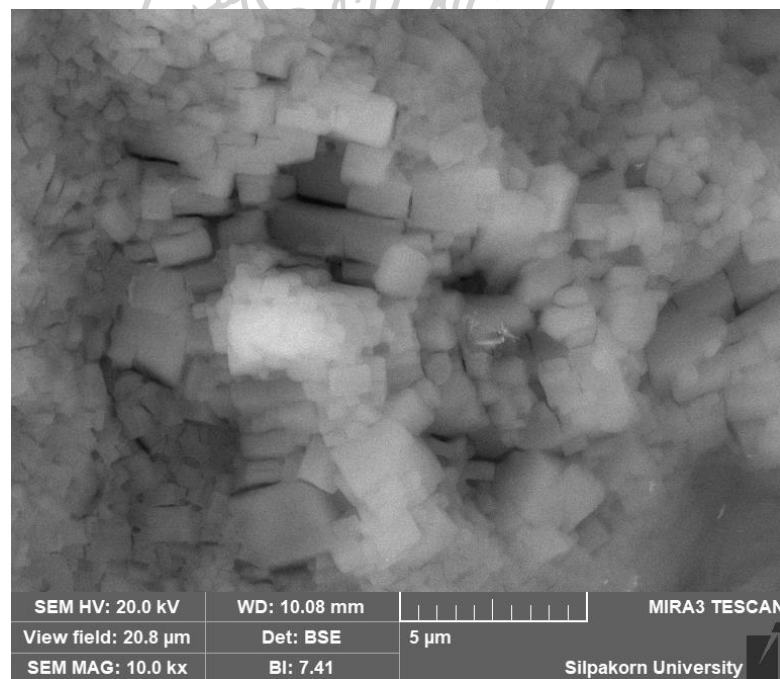
(a.) 500x magnification
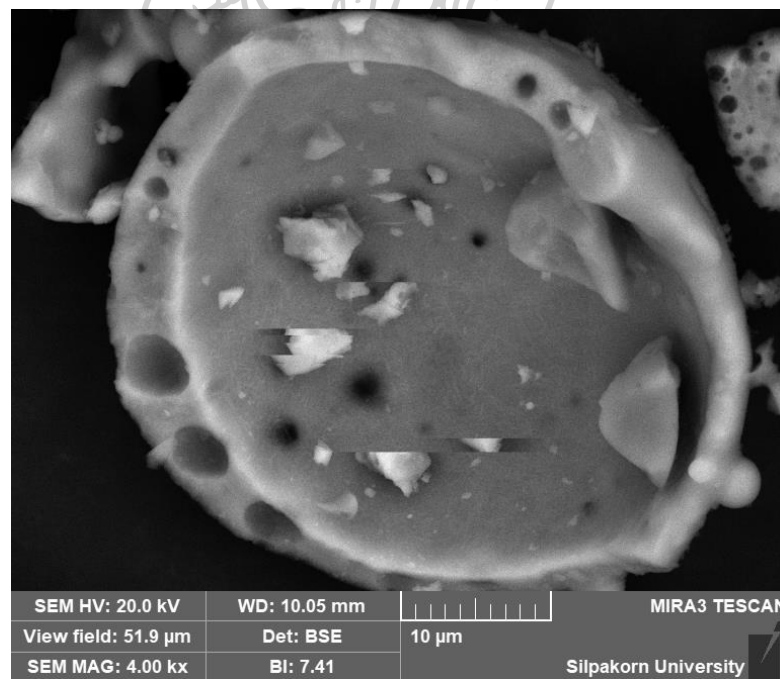
(b.) 4000x magnification

Figure 15 *The morphology of bottom ash pictured by SEM, (a.) 500x magnification, (b.) 4000x magnification*

(a.) 500x magnification

(b.) 4000x magnification

Figure 16 *The morphology of trisodium phosphate pictured by SEM, (a.) 500x magnification,*

(b.) 4000x magnification

5.2 The effect of trisodium phosphate loadings

5.2.1 XRD

The XRD patterns of all catalysts in this part were the same, as showed in Figure 17. The peaks of trisodium phosphate were observed in the range of 30°-35° and the height of the peak depends on the amount of trisodium phosphate loading. However, the patterns of XRD showed the pattern of mullite, quartz, and sodium phosphate which were referred from JCPDS no. 79-1454, 83-0539, and 30-1233.
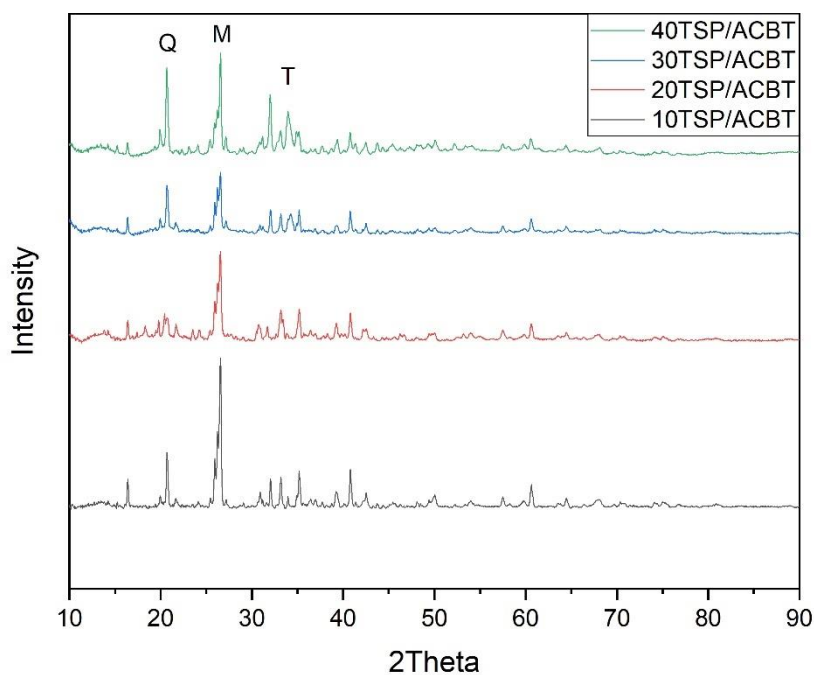

Figure 17 The XRD pattern of catalyst using various trisodium phosphate loading

5.2.2 SEM

Figure 18 showed the morphology of all catalysts using various trisodium phosphate loading. The crystal growth of trisodium phosphate can be noticed on the surface of bottom ash. At high loading of trisodium phosphate, most surface of bottom ash was covered by trisodium phosphate.
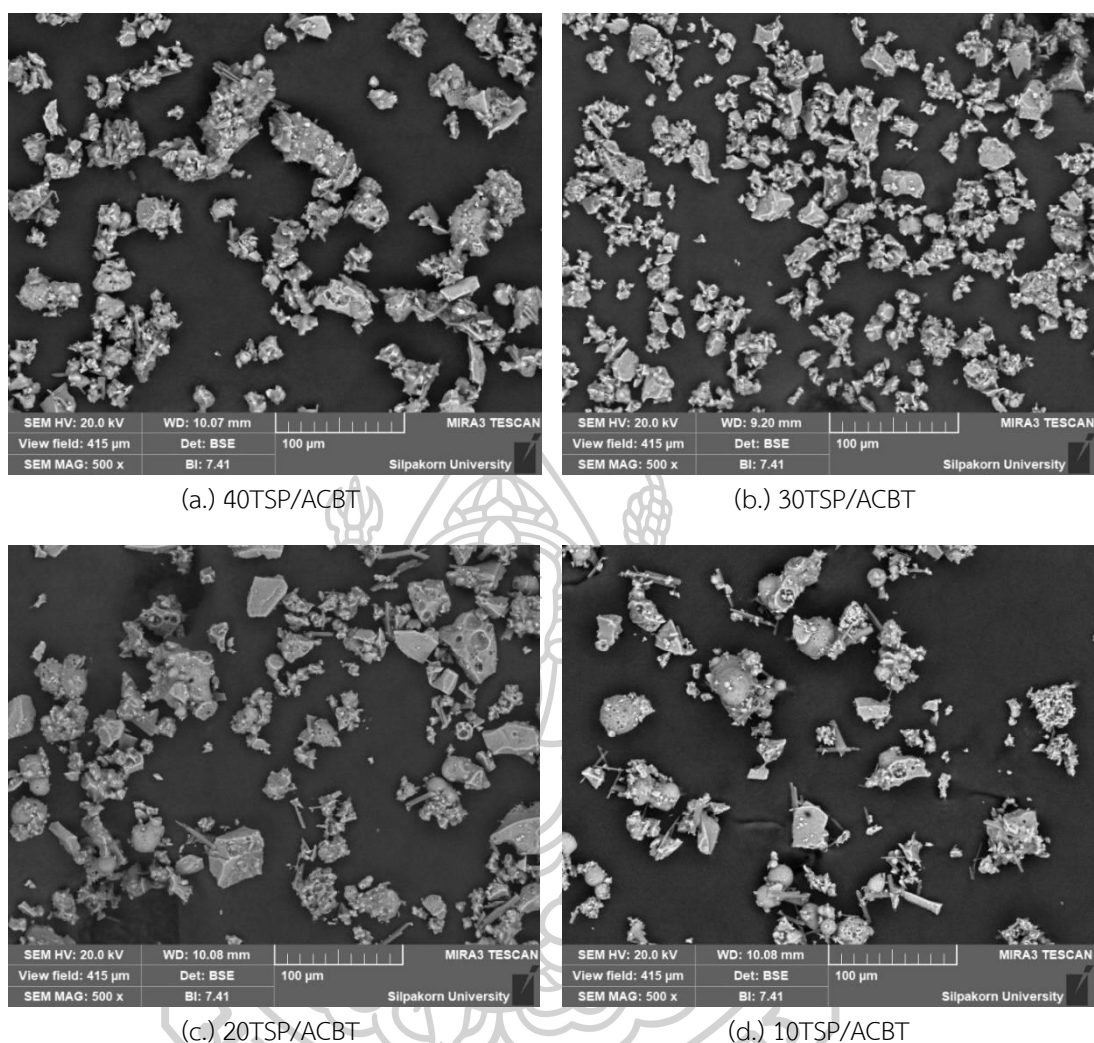
(a.) 40TSP/ACBT

(b.) 30TSP/ACBT

(c.) 20TSP/ACBT

(d.) 10TSP/ACBT

Figure 18 *The morphology of the catalysts using various trisodium phosphate loading, pictured by SEM at 500x magnification, (a.) 40TSP/ACBT, (b.) 30TSP/ACBT, (c.) 20TSP/ACBT (d.) 10TSP/ACBT*

5.2.3 BET

For BET measurement, all catalysts were characterized using N_2-physisorption. Table 10 presented the surface area and mean pore diameters of catalysts which were impregnated with different loading of trisodium phosphate.

Table 10 Surface area and mean pore size of catalysts using different percentage of TSP loadings

Catalysts	Surface area (m^2/g)	Pore size (nm)
ACBT	5.45	5.25
10TSP/ACBT	5.41	6.46
20TSP/ACBT	5.48	6.91
30TSP/ACBT	5.59	6.54
40TSP/ACBT	6.18	7.18

The surface area of catalyst slightly increased when TSP loadings increased. This might be that the active site (TSP) dispersed on the surface of the support (bottom ash). In addition, TSP loadings might affect to the structure of the bottom ash because pore size of catalyst increased. The highest surface area and the largest pore size were obtained from 40TSP/ACBT catalyst.

5.2.4 CO_2-TPD

Figure 19 showed the graph of CO_2-TPD of bottom ash. No peak occurs in this graph. This implied that the bottom ash did not have base sites because CO_2 cannot be adsorbed on the surface of bottom ash.

Figure 20 showed the graph of CO_2-TPD of catalysts which used various trisodium phosphate loadings. The peaks of CO_2-TPD occurred in the temperature range of 100-230 °C, indicating that the type of basicity of catalyst was weak base. The basicity of catalysts which loaded with TSP in different percentages were showed in Table 11, compared to the pure TSP. From the results, the basicity of catalysts depended on TSP loadings because TSP provided base site of catalyst. When TSP loading was increased, the basicity of catalyst was also increased.
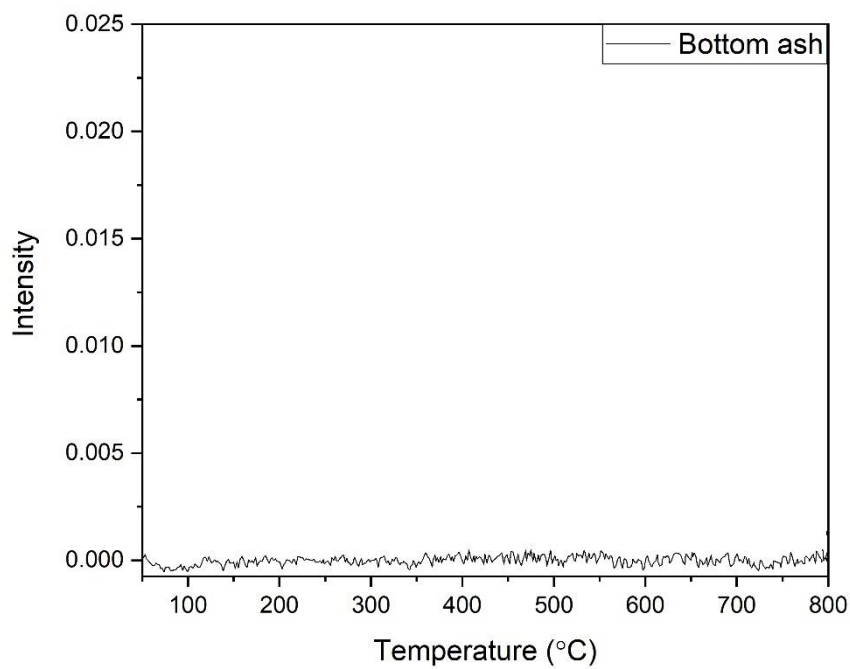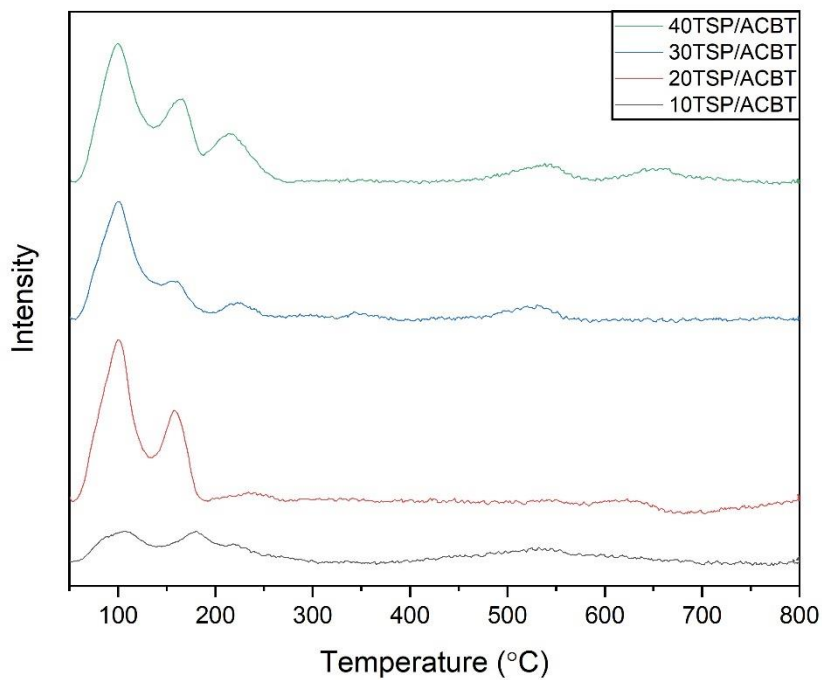
Figure 19 *CO$_2$-TPD of bottom ash*

Figure 20 *CO$_2$-TPD of catalysts using 10, 20, 30 and 40% TSP loadings*

Table 11 *The basicity of catalyst from various TSP loadings*

Catalysts	Basic sites (mmol/g)	Basicity (compared to pure TSP) (%)
TSP	6.30	100
10TSP/ACBT	1.103	25.55
20TSP/ACBT	2.198	34.89
30TSP/ACBT	2.195	34.83
40TSP/ACBT	3.733	59.25

5.2.5 GC-FID analysis

As seen in Figure 21, bottom ash without TSP impregnation cannot catalyse to produce biodiesel because pure bottom ash did not have basicity. Therefore, %FAME from the use of bottom ash was not found (0% FAME). The highest %FAME of 90.26% was obtained using 40TSP/ACBT as the catalyst. The use of 30, 20 and 10% TSP loading provided 83, 78.38, and 59.14% FAME, respectively. The trend of %FAME was similar to that of the basicity of the catalysts [56]. Higher basicity of the catalyst provided more base sites of catalysts. Therefore, it helped to catalyse transesterification reaction for biodiesel production. As the results, 40TSP/ACBT which showed the highest basic sites offered the highest %FAME, compared to other TSP loadings.
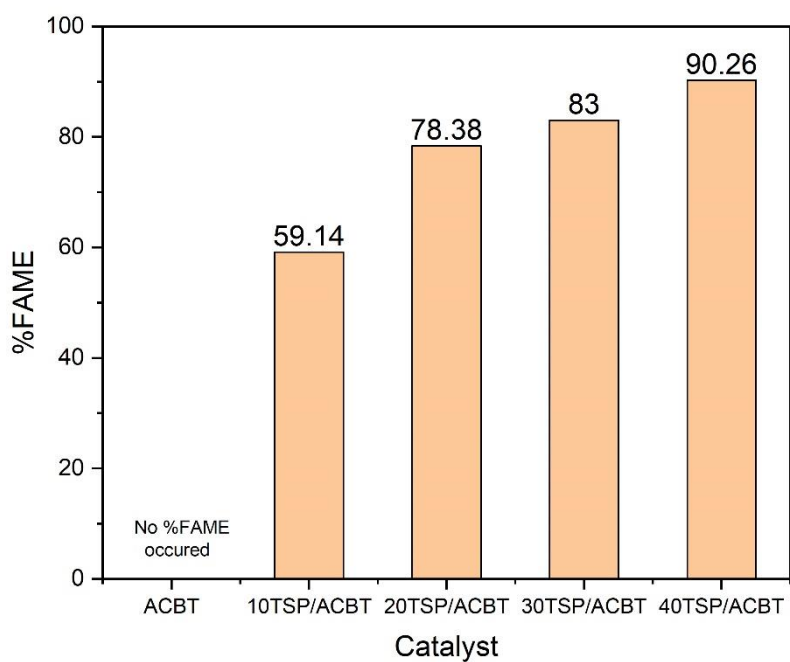
Figure 21 *The amount of methyl ester using 10, 20, 30 and 40% TSP loadings*

5.3 The effect of impregnation temperatures

5.3.1 XRD

The XRD patterns of catalysts using various impregnation temperatures were showed in Figure 22. The XRD patterns were similar to those in Figure 17 which consisted of mullite, quartz, and trisodium phosphate peaks.
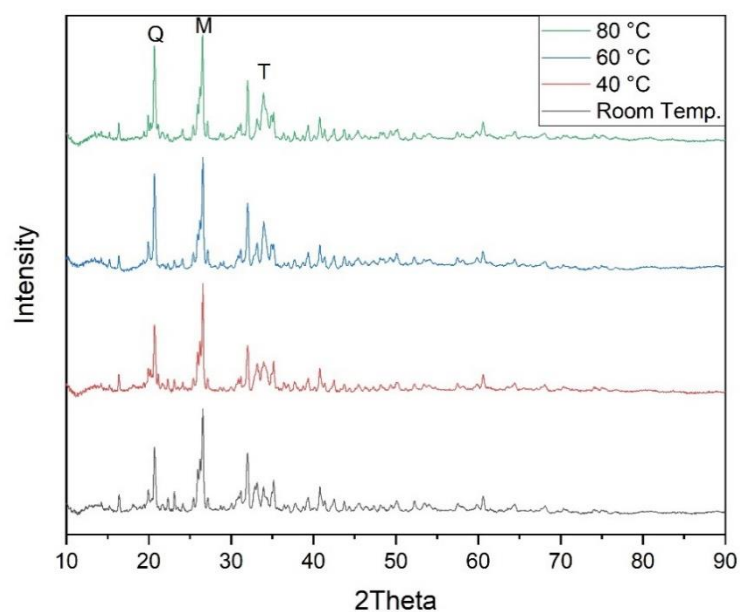
Figure 22 *The XRD patterns of catalysts using various impregnation temperatures*

5.3.2 SEM

The morphology of the catalysts using different impregnation temperatures can be seen in Figure 23. The impregnation temperature might affect to the aggregation of the catalysts. At high impregnation temperatures (60 and 80 °C), the levels of aggregation of catalysts were lower than those of lower impregnation temperatures (room temperature and 40 °C). At low impregnation temperatures, the growth of trisodium phosphate crystal can be continually proceeded. The crystal of trisodium phosphate can attached each other, increasing the aggregation of the catalysts. In contrast, trisodium phosphate can be well dispersed into the bottom ash due to high impregnation temperature. Therefore, the level of aggregation of catalysts at high impregnation temperature was less than that at low impregnation temperature.

(a.) 80 ℃
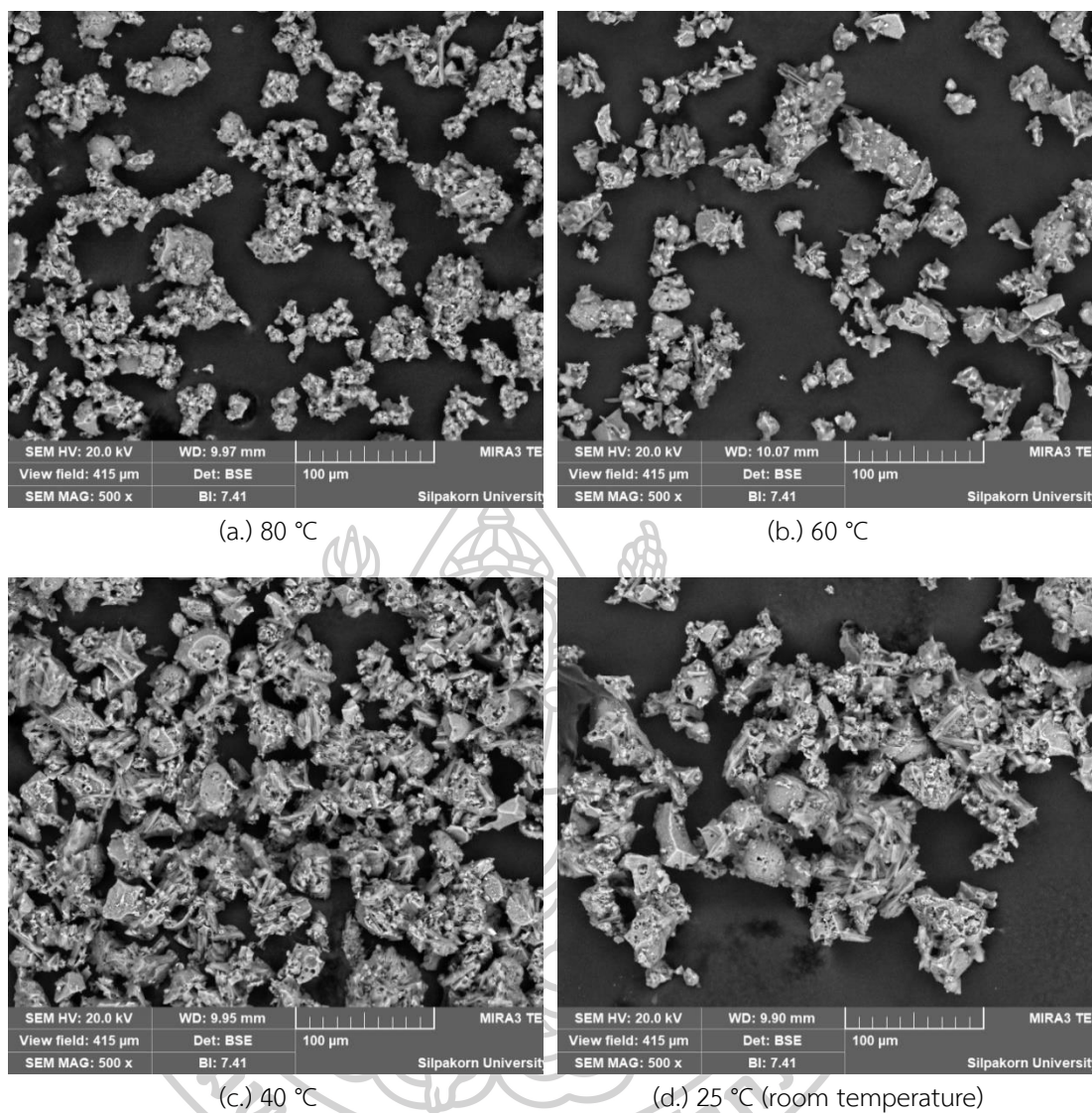
(b.) 60 ℃

(c.) 40 ℃

(d.) 25 ℃ (room temperature)

Figure 23 *The morphology of catalysts using different impregnation temperature, pictured at 500x magnification from SEM, (a.) 80 ℃, (b.) 60 ℃, (c.) 40 ℃, and (d.) 25 ℃ (room temperature)*

5.3.3 BET

The surface areas and pore sizes of the catalysts using different impregnation temperatures were showed in Table 12. The impregnation temperatures may affect to surface area of catalysts. The highest surface area was obtained from impregnation temperature of 80 °C and the largest pore size was obtained from the impregnation temperature of 60 °C. At low impregnation temperatures (room temperature and 40 °C), the residual amount of water after impregnation was still much and trisodium phosphate (active site) was still dissolved in the mixture. Therefore, TSP might not be well dispersed into the pore of bottom ash. After the impregnated catalysts were dried in the oven, trisodium phosphate might clump together into larger crystals which can block the pore of catalysts. Therefore, the pore size and surface area at low impregnation temperatures were less than those of high impregnation temperatures. Compared to high impregnation temperatures (60 °C and 80 °C), trisodium phosphate can fairly disperse into the pore of bottom ash at the beginning of the impregnation. At the end of impregnation, the residual amount of water was less. The mixture showed mud-like appearance with high viscosity. However, less trisodium phosphate was dissolved in the mixture. Therefore, there were less trisodium phosphate crystals after drying process. As the results, less crystals blocked the bottom ash pores, leading to higher surface area and larger pore size.

Table 12 *The surface area and pore size of catalysts using different impregnation temperatures*

Impregnation temperatures	Surface area (m^2/g)	Pore size (nm)
Room temperature (25 °C)	5.22	5.77
40 °C	5.21	5.69
60 °C	6.18	7.18
80 °C	6.36	6.83

5.3.4 CO$_2$-TPD

The basicity of catalysts was characterized using the same method in 5.2.2. The results showed that higher impregnation temperature contained greater basicity of the catalysts, as seen in Table 13. At higher impregnation temperatures, trisodium phosphate can transfer into the pore of bottom ash more effective than those at lower impregnation temperatures. In addition, impregnation temperature affected to the evaporation of the mixture. The water at higher impregnation temperatures (60 and 80 °C) was evaporated with higher evaporation rate than those of lower impregnation temperatures (room temperature and 40 °C). This increased the viscosity of the mixture between bottom ash and trisodium phosphate since the mixture contained lesser amount of water by increasing time. Therefore, the active site (TSP) had higher chance to attach on the support (bottom ash) at high viscosity, compared to low viscosity (higher content of water in the mixture). Thus, basicity of the catalysts at the higher impregnation temperatures was higher than those of lower impregnation temperatures. The peaks in Figure 24 occurred in range of 100-220 °C which showed the basicity of catalysts, indicating to the weak base.
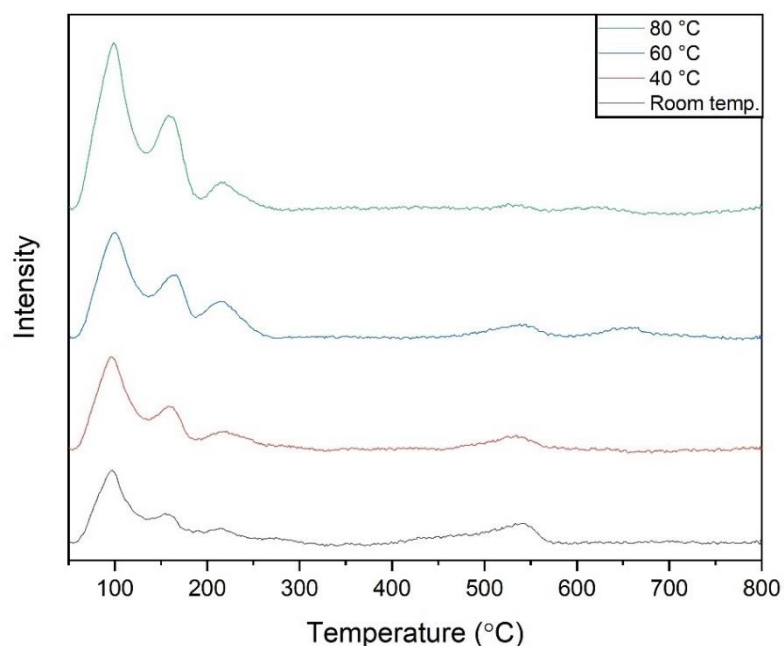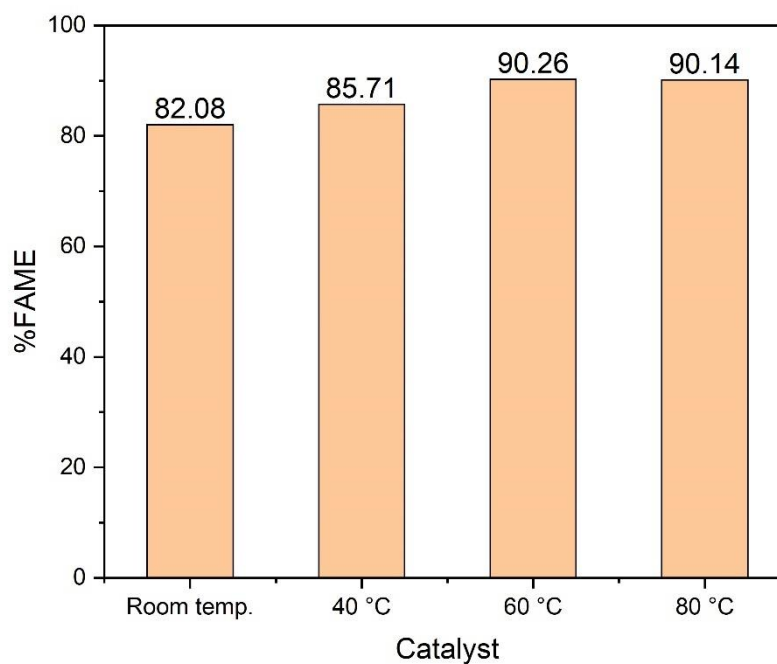

Figure 24 *CO$_2$-TPD of catalysts using different impregnation temperatures*

Table 13 The basicity of catalysts using different impregnation temperatures

Catalysts	Basic sites (mmol/g)	Basicity (compared to pure TSP) (%)
TSP	6.30	100
25 °C (room temperature)	2.203	34.98
40 °C	2.389	37.92
60 °C	3.733	59.25
80 °C	3.912	62.10

5.3.5 GC-FID analysis

As seen in Figure 25, the highest %FAME of 90.25% was observed using impregnation temperature of 60 °C. At impregnation temperature of 80 °C, %FAME of 90.14% was obtained which was slightly lower than that of 60 °C. The use of high impregnation temperatures provided the large amount of basic sites of the catalysts, as mentioned in Table 5.8. Therefore, high %FAME can be achieved using high impregnation at 60 and 80 °C.

Figure 25 The amount of methyl ester using different impregnation temperatures

5.4 The effect of calcination temperatures

5.4.1 XRD

The XRD patterns of all catalysts using various calcination temperatures were presented in Figure 26. The XRD patterns were similar to Figure 17 which consisted of mullite, quartz, and trisodium phosphate peaks.
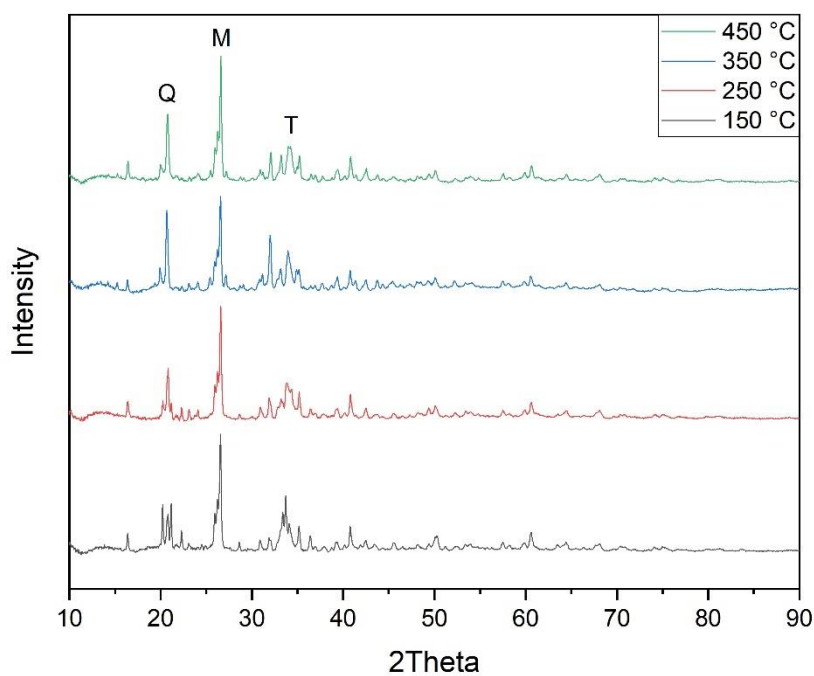
Figure 26 *The XRD patterns of catalysts using various calcination temperatures*

5.4.2 SEM

The morphology of catalysts using various calcination temperatures was showed in Figure 27 and 28, pictured at 500x and 4000x magnification by SEM.
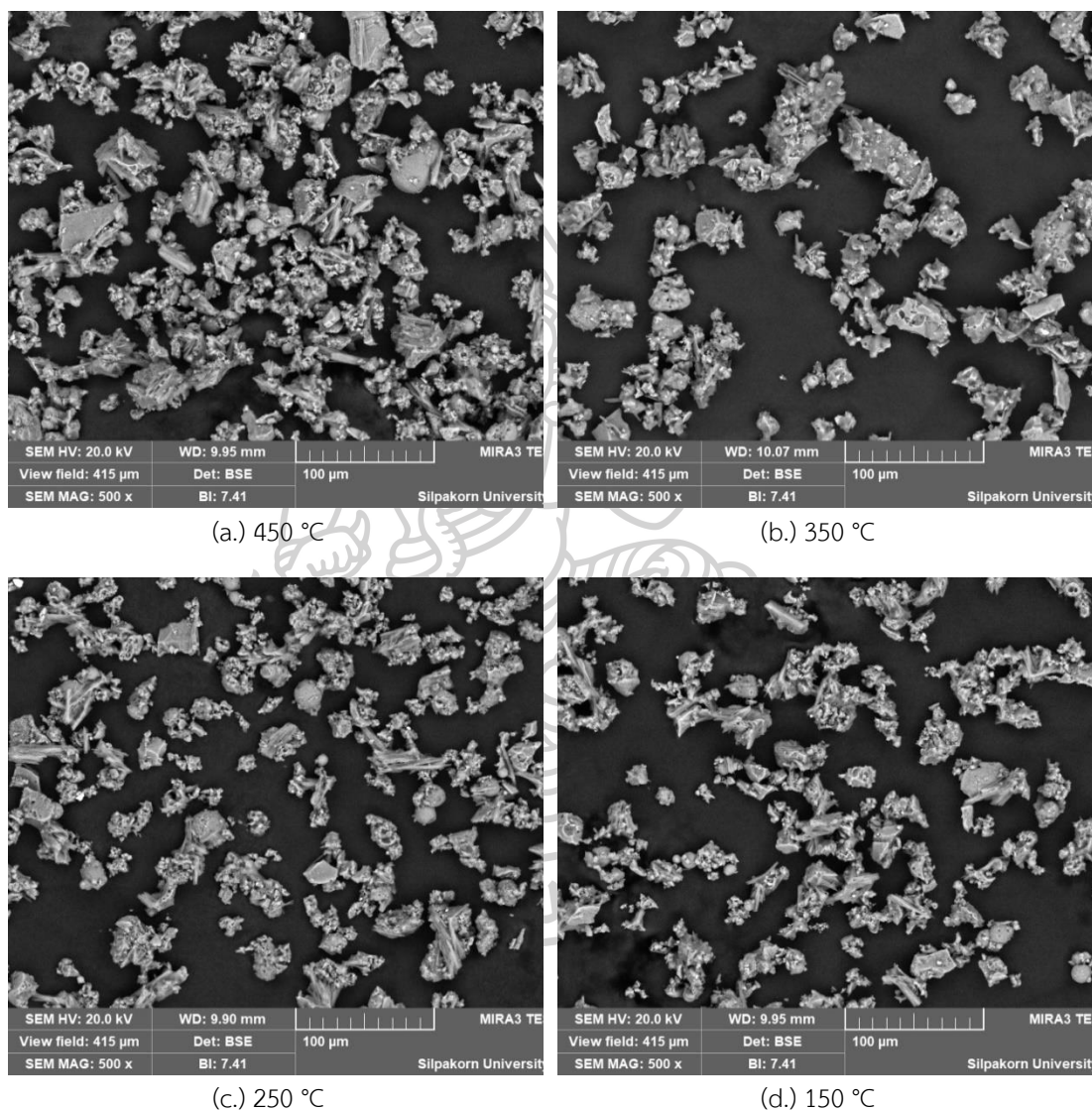

(a.) 450 ℃   (b.) 350 ℃

(c.) 250 ℃   (d.) 150 ℃

Figure 27 *The morphology of catalysts using various calcination temperatures, pictured at 500x magnification by SEM, (a.) 450 ℃, (b.) 350 ℃, (c.) 250 ℃, (d.) 150 ℃*
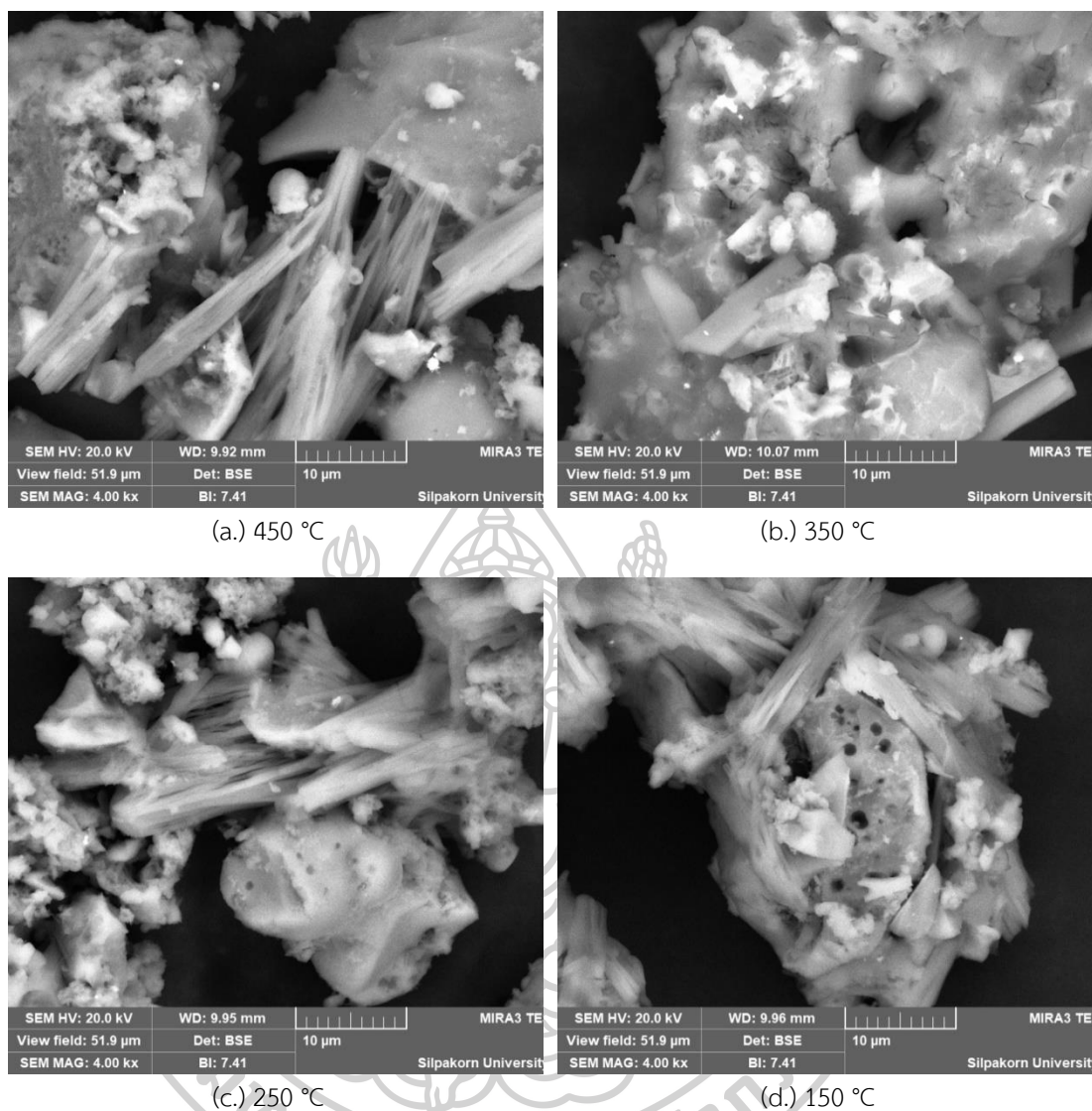
Figure 28 *The morphology of catalysts using various calcination temperatures, pictured at 4000x magnification by SEM, (a.) 450 ℃, (b.) 350 ℃, (c.) 250 ℃, (d.) 150 ℃*

5.4.3 BET

The catalysts using different calcination temperatures were characterized using N_2-physisorption, as seen in Table 14. From calcination temperatures of 150 to 350 ℃, the surface area increased from 4.85 to 6.18 m^2/g. The increase of calcination temperatures can remove more water in the crystal of trisodium phosphate, resulting to higher physisorption. Therefore, the surface area increased. However, the surface area at calcination temperature of 450 °C decreased to 5.04 m^2/g. At high calcination

temperature, the active site (TSP) of catalyst might be agglomerated. The agglomeration of TSP can block some pores of catalyst. As the result, the catalyst using calcination temperature of 450 °C showed lower surface area and smaller pore size, compared to that of 350 °C [57].

*Table 14* *The surface area and pore size of catalyst using various calcination temperatures*

Catalysts	Surface area (m^2/g)	Pore size (nm)
150 °C	4.85	5.77
250 °C	5.48	5.69
350 °C	6.18	7.18
450 °C	5.04	6.84

5.4.4 CO_2-TPD

The basicity of catalysts using various calcination temperatures was presented in Table 15. The highest basicity of the catalyst was obtained using calcination temperature of 350 °C. At lower calcination temperature such as at 150 and 250 °C, less basicity of the catalyst was observed. The crystals of active site (trisodium phosphate) might contain some water content in the structure, measured using TGA analysis as seen in Figure 30 (obtained from Okoye et al. research [18]). The presence of water might cover the base site on the surface. This led to lower basicity of the catalyst. From TGA thermogram of trisodium phosphate at zone 1 and 2 in Figure 30, the weight of trisodium phosphate dropped around 75 and 280 °C which was assigned to the water removal from crystal and the loss of volatile compounds from trisodium phosphate. At calcination temperature of 450 °C, the basicity considerably decreased, compared to that of 350 °C. The high calcination temperature might destroy the catalyst structure [58] or promote the agglomeration of active sites which was correspond to BET analysis [57]. As the result, the catalyst using calcination temperature of 450 °C provided less activity due to less basicity. The type of basicity was the same as seen in the previous section which was weak base, as illustrated in Figure 29.

Table 15 *The basicity of catalysts using different calcination temperatures*

Catalysts	Basic sites (mmol/g)	Basicity (compared to pure TSP) (%)
TSP	6.30	100
150 °C	2.421	38.44
250 °C	2.733	43.38
350 °C	3.733	59.25
450 °C	1.739	27.6
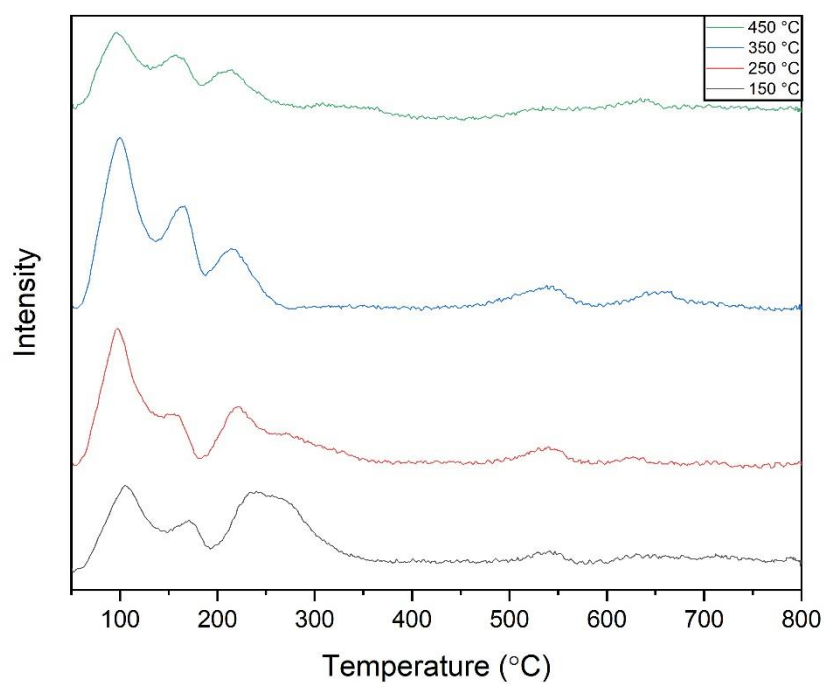
Figure 29 CO_2-*TPD of catalysts using different calcination temperatures*
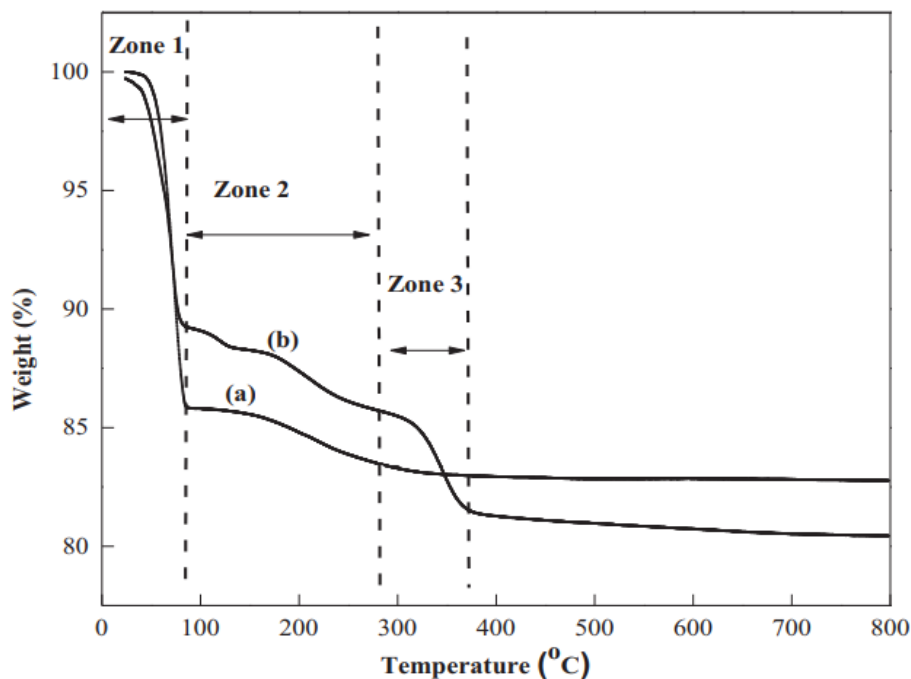
Figure 30 *TGA thermogram of (a) Fresh TSP and (b) Reused TSP for 9 times [18]*
Source: Okoye et al. (2016)

5.4.5 GC-FID analysis

From Figure 31, the catalysts using calcination temperature of 350 °C provided the highest %FAME. The trend of %FAME using different calcination temperatures corresponded to the trend of basicity. As mentioned in the previous section, the use of low calcination temperatures (150 and 250 °C) cannot remove all of the water content in the crystal. The presence of water might cover the active site of the catalysts. In addition, the catalyst structure might be destroyed at high calcination temperature of 450 °C. These resulted in lower basicity of the catalyst. Therefore, less %FAME was observed at low and high calcination temperatures.

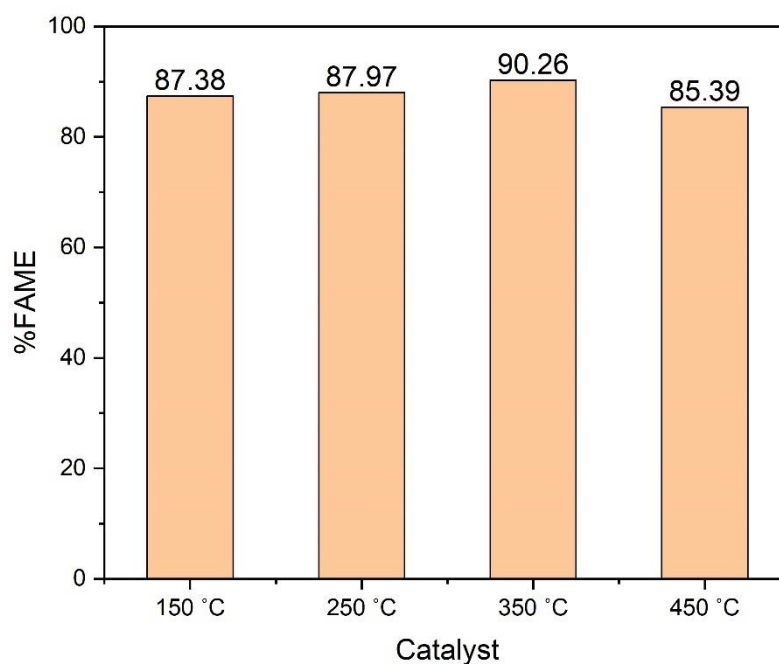*Figure 31* *The amount of methyl ester using different calcination temperatures*

5.5 Box-Behnken design

This section showed the Box-Behnken experimental design to find the optimized catalyst synthesis conditions. The variables used were trisodium phosphate loadings, impregnation temperatures and calcination temperatures. The response of experimental design was presented in Table 16.

Table 16 *The response of experimental design*

No.	Factor			%FAME
	TSP loadings	Impregnation temperatures	Calcination temperatures	
1	20 (-1)	40 (-1)	350 (0)	71.17
2	40 (1)	40 (-1)	350 (0)	85.72
3	40 (1)	80 (1)	350 (0)	90.14
4	40 (1)	60 (0)	250 (-1)	87.97
5	20 (-1)	60 (0)	250 (-1)	61.66
6	30 (0)	40 (-1)	250 (-1)	80.88
7	20 (-1)	60 (0)	450 (1)	68.75
8	30 (0)	60 (0)	350 (0)	83.00
9	40 (1)	60 (0)	450 (1)	85.39
10	30 (0)	40 (-1)	450 (1)	83.09
11	30 (0)	60 (0)	350 (0)	83.00
12	30 (0)	80 (1)	450 (1)	70.01
13	30 (0)	60 (0)	350 (0)	83.00
14	20 (-1)	80 (1)	350 (0)	80.71
15	30 (0)	80 (1)	250 (-1)	82.94

The optimum %FAME was 90.14% (observed in No.3) while the minimum %FAME was 61.66% (observed in No.5). For the experiment No.3 (optimum %FAME), the catalyst synthesis conditions were trisodium phosphate loading (1), impregnation temperature (1) and calcination temperature (0). The catalyst synthesis conditions from the experiment No.5 (minimum %FAME) were trisodium phosphate loading (-1), impregnation temperature (0) and calcination temperature (-1). The level of TSP loading variables was very different so that this variable was strongly effective to %FAME. However, the level of other variables was different around 1 level so that those variables were slightly effective to %FAME.

The result of experiment was analyzed using Minitab program and the prediction equation was calculated in the form of full quadratic model which consisted

of several terms of constants, linear, quadratic, and interaction [59]. The correlation equation of variables was presented as seen in the equation below.

$$\%FAME = -86.5 + 3.37\ A + 0.54\ B + 0.520\ C - 0.0218\ A^2 + 0.00277\ B^2$$
$$- 0.000488\ C^2 - 0.0064\ AB - 0.00242\ AC - 0.00189\ BC$$

where   A   is trisodium phosphate loading

          B   is impregnation temperature

          C   is calcination temperature

Next, the coefficient was discussed using p-value to define the significance of variables to %FAME. Normally, p-value should be less or equal 0.05 because it provides 95% confident level of variable. If p-value is more than 0.05, it indicates that this variable is not significant to the response at the confident level of 95% [60]. Therefore, if the variable has less p-value, this variable has more effect to the response (%FAME). The p-value was shown in Table 17.

Considering about coefficient in every term, the confident level of significance can be ordered as follows; calcination temperatures, TSP loadings and impregnation temperatures, respectively.

Table 17 The coefficient values and p-values from correlation equation

Factor	Coefficient	p-value
Constant	-86.5	0.278
A	3.37	0.177
B	0.54	0.637
C	0.52	0.076
A^2	0.0218	0.482
B^2	0.00277	0.715
C^2	0.000488	0.150
AB	0.0064	0.663
AC	0.00242	0.421
BC	0.00189	0.228

The interactions between variables and the responses were showed in Figure 32. The trend of graph can determine the effect of variables to the response (%FAME). The increase of TSP loading strongly affects to the increase of %FAME, while the impregnation temperatures were not strongly significant to %FAME. For the last variable, the calcination temperature had the optimum point at 350 ℃. It demonstrated that increasing calcination temperature was more effective until the calcination temperature of 350 ℃. Also, it became less effective if the calcination temperature was higher than 350 ℃ as %FAME decreased.

Figure 32 *The main effect plot for %FAME*
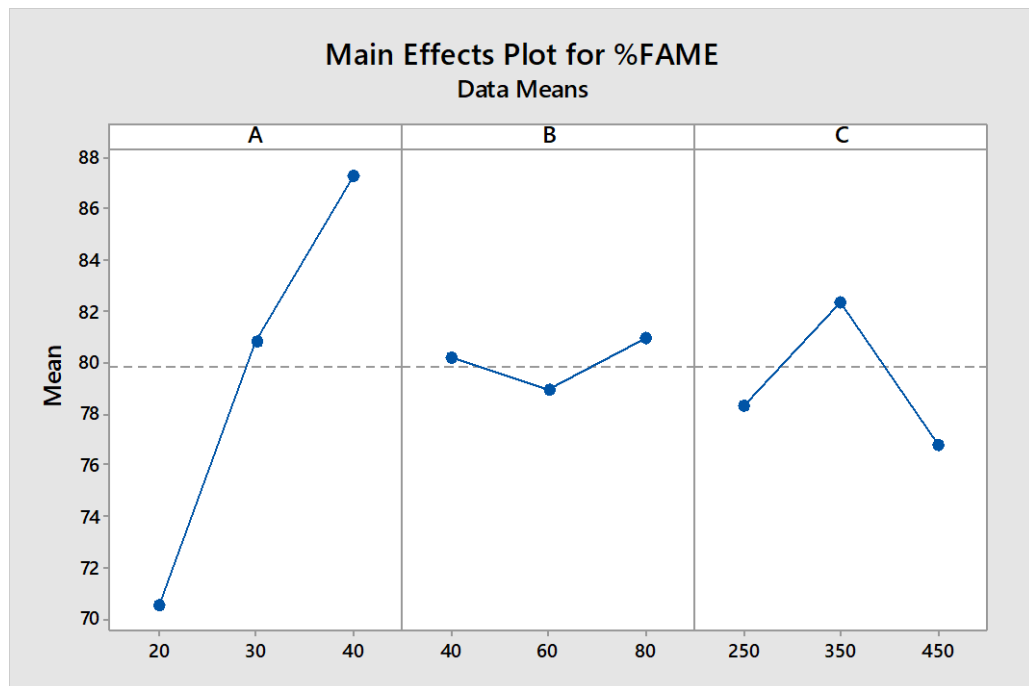
In addition, this section will find the optimum condition from Box-Behnken experimental design. From the use of the Minitab optimizer, the best conditions of catalyst synthesis were obtained when using TSP loading of 40 wt%, impregnation temperature of 80 °C and calcination temperature of 278 °C, as seen in Figure 33.
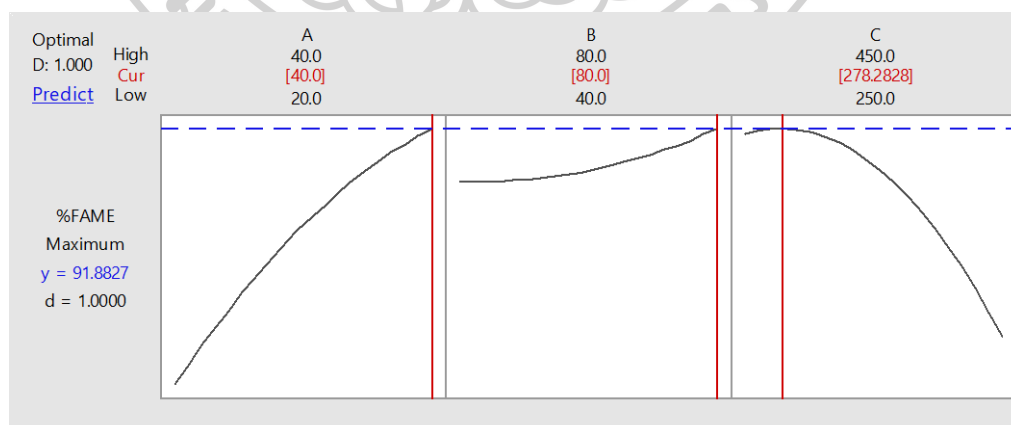

Figure 33 *The minitab optimizer of catalyst synthesis condition*

As seen in Figure 33, the highest %FAME was predicted at 91.88%, using Minitab optimizer. Next, the catalyst was synthesized under conditions from Minitab optimizer and tested for biodiesel reaction, using methanol to oil ratio of 15:1, stirring speed of 600 rpm and reaction temperature of 60 °C for 3 hours. The results illustrated that %FAME of 93.03% was obtained. This value was close to the predicted %FAME of 91.88% (error 1.24%). The %FAME of 93.03% which used catalyst prepared from Minitab optimizer condition was higher than those of predicted value (91.88%) and previous prepared catalyst (90.26%), respectively.

5.6 The effect of methanol to oil ratios

This section aimed to find the suitable methanol to oil ratios for biodiesel production, using Box-Behnken experimental design. The methanol to oil ratio is one of important factors for reaction condition. The catalyst was prepared using the TSP loading of 40%, impregnation temperature of 80 °C and calcination temperature of 278 °C. The results of %FAME were presented in Table18.

Table 18 %FAME using different ratios of methanol to oil

Methanol to oil ratio	%FAME
9:1	83.40
12:1	87.50
15:1	93.03
18:1	93.69

The trend of %FAME was similar to the trend of methanol to oil ratio. The higher methanol to oil ration can increase %FAME. Normally, the stoichiometric methanol to oil ratio for transesterification reaction is 3:1. The excess of methanol using high methanol to oil ratio improved the contact between phases of methanol, oil, and catalyst [61]. From the use of methanol to oil ratio of 15:1 and 18:1, %FAME from both ratios were similar. However, higher methanol to oil ratio than 18:1 might

not increase more %FAME as the transesterification reaction can be reversible at high ratio of methanol to oil.

5.7 Reusability of catalyst

The reusability of catalyst was investigated in this section. The characterization of the catalyst was carried out before and after the reaction.

From the previous section, the catalyst prepared using Box-Behnken optimizer condition can provide %FAME of 93.69%. After the reaction, the catalyst was washed using methanol and then was used for catalysis again. The result showed that catalyst was deactivated. There was no %FAME observed from reused catalyst. After separation process, the reused catalyst was washed again using methanol. The reused catalyst after the second round of reaction was characterized using BET and CO_2-TPD techniques. The properties of catalyst were showed in Table 19.

Table 19 The properties of catalyst before and after the reaction

Properties	Catalysts	
	Before (1st round)	After (2nd round)
Surface area	5.71	4.40
Pore size	6.65	4.21
Basicity (compared to TSP) (%)	43.19	8.99

The graphs of CO_2-TPD of catalysts in comparison between before (1st round) and after (2nd round) reaction can be seen in Figure 34 and 35. For Figure 34, CO_2 desorption occurred in temperature range of 100-200 °C. It implied that the basicity of catalyst was weak base. However, after the use of catalyst at 2nd round, the peaks occurred in the range of 350-550 °C, as seen in Figure 35. These peaks might not be CO_2 desorption of the catalyst. They might be from CO_2 desorption of the residual oil in the catalyst. After CO_2-TPD characterization, the catalyst appearance can be seen in Figure 36. The catalyst looked burned. This might be the presence of oil inside the

catalyst. The residual oil cannot be completely removed out of the catalyst using pure methanol several times. Therefore, the residual oil in the catalyst can be burned since CO_2-TPD measurement was carried out at high temperature, resulting to black powder of catalyst.

In addition, the used catalyst was washed several times using methanol, and then calcined at 350 °C for 2 hours in order to remove residual oil. The catalyst was then measured using CO_2-TPD technique, as seen in Figure 37. There were no peaks observed in the graph. It demonstrated that the catalyst lost basic sites after the first round of transesterification reaction. The reusability of the catalyst in this work was not achieved. The further study to improve reusability of the catalyst should be investigated in the future.
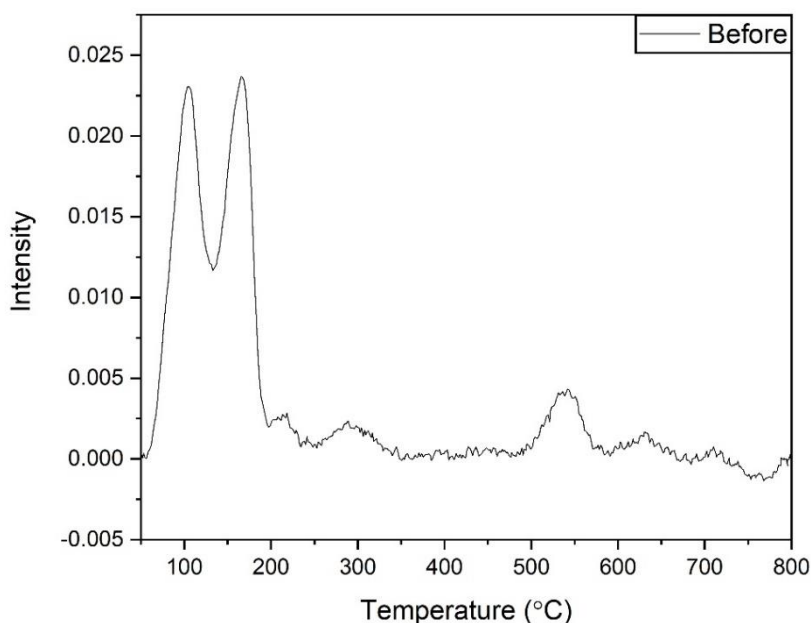

Figure 34 *CO_2-TPD of catalyst from Box-Behnken design conditions before use (1st round)*
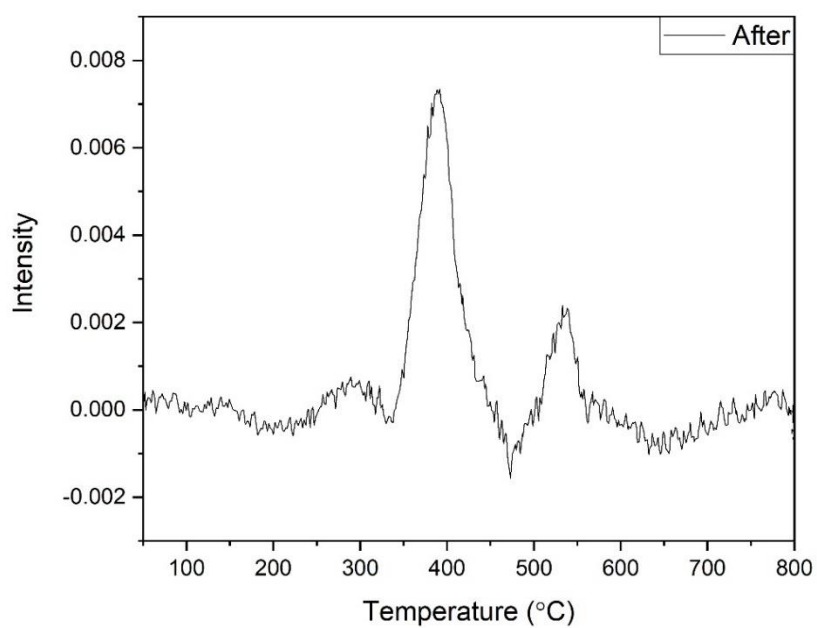
Figure 35 *CO_2-TPD of catalyst from Box-Behnken design conditions after use (2nd round)*

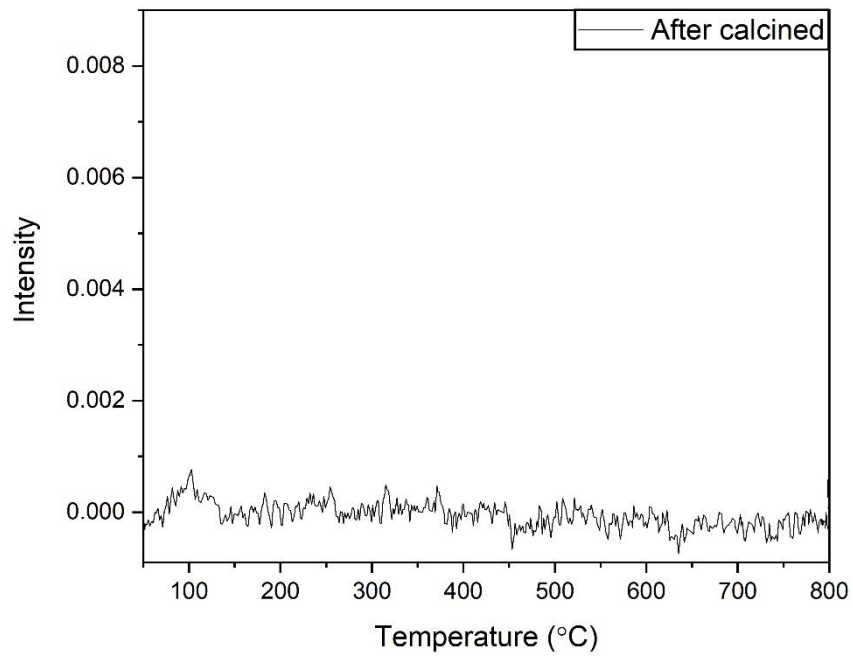***Figure 36*** *The appearance of the catalyst after CO_2-TPD measurement*

Figure 37 *CO_2-TPD of catalyst from Box-Behnken design conditions after use and calcination*

Chapter 6 Conclusion

This chapter summarizes all parts of this work such as the effect of TSP loadings, impregnation temperatures and calcination temperature, including the use of design of experiment (Box-Behnken design) to support the results in the experiment. The recommendation for this work was also included in this chapter.

6.1 Conclusion

In this work, trisodium phosphate (TSP) was impregnated on bottom ash, using incipient wetness impregnation method for the use as the catalyst in transesterification reaction. For various TSP loadings of 10%, 20%, 30%, and 40%, %FAME was more increased when higher TSP loading was applied. Higher TSP loading increased the basicity of the catalyst which provided more active sites to catalyze transesterification reaction, providing higher %FAME. The effect of impregnation temperatures was not much influent to %FAME. At low impregnation temperatures (room temperature of 25 °C and 40 °C), the dispersion of active sites was not good as that of high impregnation temperatures (60 and 80 °C). The amount of residual water at low impregnation temperatures was still too much and active sites (TSP) were still dissolved in the mixture. After drying in an oven, active sites can be agglomerated and can block the pore of bottom ash. As the result, this led to less surface area and smaller pore size which was not useful for good dispersion of active sites. Therefore, good dispersion of active sites was observed using high impregnation temperatures, leading to high basicity of the catalyst.

For the effect of calcination temperatures, it affected the structure and composition of the catalysts. The catalysts which were calcined at 150 and 250 °C still contained the water in the crystal of TSP. However, high calcination temperature of 450 °C, the agglomeration of active sites was noticed, leading to less basicity of catalyst

due to less surface area. Therefore, the calcination temperature of 350 °C provided highest basicity of catalyst and %FAME.

The previous results mentioned above corresponded to the results using Box-Behnken experimental design. The Box-Behnken analysis demonstrated that the response (%FAME) was strongly influenced with high TSP loadings, high impregnation temperature and calcination temperature of 350 °C. The optimum conditions of catalyst synthesis were found using Minitab optimizer which the catalysts was impregnated using TSP loading of 40%, impregnation temperature of 80 °C and calcination temperature of 278 °C.

In addition, the methanol to oil ratios were studied using various ratios at 9:1, 12:1, 15:1, and 18:1. At the methanol to oil ratio of 18:1 was the best ratio in the experiment. For the reusability of the catalyst, it showed that the catalyst did not provide the reusability property since the active sites of the catalyst were leached out. The catalysts were then deactivated.

6.2 Recommendation

6.2.1 The study on the prevention of catalyst deactivation should be further carried out.

6.2.2 The treatment of the bottom ash properties before impregnation process should be developed, in order to increase surface area and enhance the dispersion of active site species.

6.2.3 The rate of reaction of TSP-impregnated bottom ash should be investigated, comparing to that of trisodium phosphate in commercial grade.

6.2.4 The study on the impregnation method should be further investigated, in order to prevent the leaching of trisodium phosphate.

REFERENCES

1. DEDE. *Percentage of Alternative Energy Consumption*. 13/05/2020]; Available from:
https://www.dede.go.th/download/stat63/Percentage_of_Alternative_Energy_Consumption_January_2563.pdf.

2. EGAT. ฝุ่น *PM 2.5* มาจากไหน ต้องแก้อย่างไรให้ตรงจุด. 14/05/2020]; Available from:
https://www.egat.co.th/index.php?option=com_content&view=article&id=1749:article-20161115&catid=49&Itemid=251.

3. Zhang, J., et al., *Comparison of particle emissions from an engine operating on biodiesel and petroleum diesel.* Fuel, 2011. **90**(6): p. 2089-2097.

4. บัวศรี, อ., ไบโอดีเซล : พลังงานพอเพียง. 2555, ภาควิชาวิทยาการและวิศวกรรมวัสดุ คณะวิศวกรรมศาสตร์และเทคโนโลยีอุตสาหกรรม มหาวิทยาลัยศิลปากร.

5. EPPO. *Power Overview*. 13/05/2020]; Available from:
http://www.eppo.go.th/images/Energy-Statistics/energyinformation/Energy_Statistics/00All.pdf.

6. NST. การเปรียบเทียบข้อดีและข้อเสียของโรงไฟฟ้านิวเคลียร์กับโรงไฟฟ้าที่ใช้เชื้อเพลิงชนิดอื่น. 20/05/2020]; Available from: http://www.nst.or.th/powerplant/pp04.htm.

7. MOST/GISTDA. ไทยมี "โรงไฟฟ้าถ่านหิน" กี่แห่ง. 2017 20/05/2020]; Available from: http://coastalradar.gistda.or.th/wp/?page=news-detail&id=3956.

8. DMF. ถ่านหิน. 21/05/2020]; Available from:
https://dmf.go.th/public/list/data/index/menu/630/mainmenu/630/.

9. Chindaprasirt, P., et al., *Comparative study on the characteristics of fly ash and bottom ash geopolymers.* Waste management, 2009. **29**(2): p. 539-543.

10. Jaturapitakkul, C. and R. Cheerarot, *Development of bottom ash as pozzolanic material.* Journal of materials in civil engineering, 2003. **15**(1): p. 48-53.

11. กรมควบคุมมลพิษ. ความสำเร็จในการจัดการมลพิษของประเทศไทย. 22/05/2020]; Available from: http://www.pcd.go.th/info_serv/pol_suc_ash.html.

12. Kim, H.-K., *Utilization of sieved and ground coal bottom ash powders as a coarse binder in high-strength mortar to improve workability.* Construction and Building Materials, 2015. **91**: p. 57-64.

13. Bennett, J.A., K. Wilson, and A.F. Lee, *Catalytic applications of waste derived materials.* Journal of materials chemistry A, 2016. **4**(10): p. 3617-3637.

14. Loy, A.C.M., et al., *The effect of industrial waste coal bottom ash as catalyst in catalytic pyrolysis of rice husk for syngas production.* Energy Conversion and Management, 2018. **165**: p. 541-554.

15. Inayat, A., et al., *Parametric analysis and optimization for the catalytic air gasification of palm kernel shell using coal bottom ash as catalyst.* Renewable Energy, 2020. **145**: p. 671-681.

16. Wang, Y., et al., *Municipal solid waste incineration bottom ash supported cobalt oxide catalysts for dye degradation using sulfate radical.* Journal of the Taiwan Institute of Chemical Engineers, 2016. **68**: p. 246-253.

17. ChemicalBook. *Trisodium phosphate.* CAS DataBase 16/05/2020]; Available from: https://www.chemicalbook.com/ChemicalProductProperty_EN_cb4364607.htm.

18. Okoye, P., A. Abdullah, and B. Hameed, *Glycerol carbonate synthesis from glycerol and dimethyl carbonate using trisodium phosphate.* Journal of the Taiwan Institute of Chemical Engineers, 2016. **68**: p. 51-58.

19. Biotechnology, N.C. *Trisodium-phosphate.* 15/05/2020]; Available from: https://pubchem.ncbi.nlm.nih.gov/compound/Trisodium-phosphate.

20. Arzamendi, G., et al., *Alkaline and alkaline-earth metals compounds as catalysts for the methanolysis of sunflower oil.* Catalysis Today, 2008. **133**: p. 305-313.

21. Li, J.-T., et al., *An efficient and practical synthesis of β-hydroxyl ketones catalysed by trisodium phosphate under ultrasound.* Journal of Chemical Research, 2004. **2004**(12): p. 838-839.

22. Deraz, N., *The comparative jurisprudence of catalysts preparation methods: I. Precipitation and impregnation methods.* J Ind Environ Chem. 2018; 2 (1): 19, 2018. **21**.

23. Doswell, S. *Preparation & Characterization of heterogeneous catalyst.* 2015 22/05/2020]; Available from: https://slideplayer.com/slide/4143065/.

24.   Babajide, O., et al., *Use of coal fly ash as a catalyst in the production of biodiesel.* 2010.

25.   Bhandari, R., V. Volli, and M. Purkait, *Preparation and characterization of fly ash based mesoporous catalyst for transesterification of soybean oil.* Journal of Environmental Chemical Engineering, 2015. **3**(2): p. 906-914.

26.   Kotwal, M., et al., *Transesterification of sunflower oil catalyzed by flyash-based solid catalysts.* Fuel, 2009. **88**(9): p. 1773-1778.

27.   Manique, M.C., et al., *Biodiesel production using coal fly ash-derived sodalite as a heterogeneous catalyst.* Fuel, 2017. **190**: p. 268-273.

28.   De Filippis, P., C. Borgianni, and M. Paolucci, *Rapeseed oil transesterification catalyzed by sodium phosphates.* Energy & fuels, 2005. **19**(6): p. 2225-2228.

29.   Jiang, S., F. Zhang, and L. Pan, *Sodium phosphate as a solid catalyst for biodiesel preparation.* Brazilian Journal of Chemical Engineering, 2010. **27**(1): p. 137-144.

30.   Thinnakorn, K. and J. Tscheikuna, *Biodiesel production via transesterification of palm olein using sodium phosphate as a heterogeneous catalyst.* Applied Catalysis A: General, 2014. **476**: p. 26-33.

31.   Yatish, K., et al., *Synthesis of biodiesel from Garcinia gummi-gutta, Terminalia belerica and Aegle marmelos seed oil and investigation of fuel properties.* Biofuels, 2018. **9**(1): p. 121-128.

32.   Suksuchot, W., *Synthesis of Tri-Sodium Phosphate Derived from Thai Monazite Ore Processing as Catalyst for Transesterification*, in *Department of Chemical Engineering*. 2561, Kasetsart University.

33.   มั่งมีสิทธิ์, ส., ไบโอดีเซลชุมชนคนรากแก้ว วิถีการอยู่อย่างพอเพียง. Vol. 1. 2550, สถาบันวิจัยและพัฒนามหาวิทยาลัยศิลปากร.

34.   Ma, F. and M.A. Hanna, *Biodiesel production: a review.* Bioresource technology, 1999. **70**(1): p. 1-15.

35.   Fukuda, H., A. Kondo, and H. Noda, *Biodiesel fuel production by transesterification of oils.* Journal of bioscience and bioengineering, 2001. **92**(5): p. 405-416.

36. รัตนพระ, ด., การตรึงไลเปสจาก *Pseudomonas fluorescens* เพื่อผลิตไบโอดีเซลจาก น้ำมันเมล็ดทานตะวัน, in ภาควิชาวิศวกรรมเคมี คณะวิศวกรรมศาสตร์. 2549, มหาวิทยาลัยเกษตรศาสตร์.

37. ดำ, ว.ค., ว.ศ.ว.ท.ร.อ.ป. ธร, and ร.ต.พ.ษ.ส. มงคล, *EFFECT OF HIGH VOLUME REPLACEMENT OF FINE AGGREGATE WITH BOTTOM ASH ON FLOW, SETTING TIME, COMPRESSIVE STRENGTH AND SHRINKAGE OF MORTAR.* Journal of Thailand Concrete Association, 2016. **4**(2): p. 1-13.

38. กฟผ. จากเถ้าหนักไร้ราคา สู่บล็อกประสานสร้างมูลค่า สร้างงาน สร้างอาชีพแก่ชุมชนแม่ เมาะ. 2018   16/05/2020]; Available from: https://www.egat.co.th/index.php?option=com_content&view=article&id=2466 :csr-20180404-01&catid=32&Itemid=169.

39. Dou, X., et al., *Review of MSWI bottom ash utilization from perspectives of collective characterization, treatment and existing application.* Renewable and Sustainable Energy Reviews, 2017. **79**: p. 24-38.

40. Herman, A.P., et al., *Bottom ash characterization and its catalytic potential in biomass gasification.* Procedia engineering, 2016. **148**: p. 432-436.

41. Shahbaz, M., et al., *Artificial neural network approach for the steam gasification of palm oil waste using bottom ash and CaO.* Renewable energy, 2019. **132**: p. 243-254.

42. CHATCHAWAN, R., *USE OF FLY ASH TO ENHANCE PERFORMANCE OF EXPANSIVE CONCRETE.* 2017, THAMMASAT UNIVERSITY.

43. Nguyen, T., W. Saengsoy, and S. Tangtermsirikul, *Influence of Bottom Ashes with Different Water Retainabilities on Properties of Expansive Mortars and Expansive Concretes.* Engineering Journal, 2019. **23**(5): p. 107-123.

44. ul Haq, E., S.K. Padmanabhan, and A. Licciulli, *Synthesis and characteristics of fly ash and bottom ash based geopolymers–A comparative study.* Ceramics International, 2014. **40**(2): p. 2965-2971.

45. Bennazha, J., et al., *Na2CaP2O7, a new catalyst for Knoevenagel reaction.* Catalysis Communications, 2001. **2**(3-4): p. 101-104.

46.   Bock, C., H. Halvorsen, and B. MacDougall, *Catalyst synthesis techniques*, in *PEM Fuel Cell Electrocatalysts and Catalyst Layers*. 2008, Springer. p. 447-485.

47.   Ferreira, S.C., et al., *Box-Behnken design: an alternative for the optimization of analytical methods.* Analytica chimica acta, 2007. **597**(2): p. 179-186.

48.   Dwivedi, G. and M. Sharma, *Application of Box–Behnken design in optimization of biodiesel yield from Pongamia oil and its stability analysis.* Fuel, 2015. **145**: p. 256-262.

49.   Hanyotee, S. and M. Chareonpenich, *Synthesis of High Purity ZSM-5 Zeolite from Lignite Fly Ash via Two-stage Process.* Engineering and Applied Science Research, 2004. **31**(4): p. 409-424.

50.   Volli, V. and M. Purkait, *Selective preparation of zeolite X and A from flyash and its use as catalyst for biodiesel production.* Journal of hazardous materials, 2015. **297**: p. 101-111.

51.   Hadiyanto, H., S.P. Lestari, and W. Widayat, *Preparation and characterization of Anadara Granosa shells and CaCO3 as heterogeneous catalyst for biodiesel production.* Bulletin of Chemical Reaction Engineering & Catalysis, 2016. **11**(1): p. 21-26.

52.   Sankaranarayanan, S., C.A. Antonyraj, and S. Kannan, *Transesterification of edible, non-edible and used cooking oils for biodiesel production using calcined layered double hydroxides as reusable base catalysts.* Bioresource technology, 2012. **109**: p. 57-62.

53.   Wei, Z., C. Xu, and B. Li, *Application of waste eggshell as low-cost solid catalyst for biodiesel production.* Bioresource technology, 2009. **100**(11): p. 2883-2885.

54.   Kawashima, A., K. Matsubara, and K. Honda, *Development of heterogeneous base catalysts for biodiesel production.* Bioresource technology, 2008. **99**(9): p. 3439-3443.

55.   Brouwer, P., *Theory of XRF.* Almelo, Netherlands: PANalytical BV, 2006.

56.   Wong, Y., et al., *Biodiesel production via transesterification of palm oil by using CaO–CeO2 mixed oxide catalysts.* Fuel, 2015. **162**: p. 288-293.

57.   Pandey, A.K. and K. Biswas, *Effect of agglomeration and calcination temperature on the mechanical properties of yttria stabilized zirconia (YSZ).* Ceramics International, 2014. **40**(9): p. 14111-14117.

58.   Sun, Q., et al., *Influence of calcination temperature on the structural, adsorption and photocatalytic properties of TiO2 nanoparticles supported on natural zeolite.* Powder Technology, 2015. **274**: p. 88-97.

59.   Hamze, H., M. Akia, and F. Yazdani, *Optimization of biodiesel production from the waste cooking oil using response surface methodology.* Process Safety and Environmental Protection, 2015. **94**: p. 1-10.

60.   Boonmee, K., et al., *Optimization of biodiesel production from Jatropha oil (Jatropha curcas L.) using response surface methodology.* Agriculture and Natural Resources, 2010. **44**(2): p. 290-299.

61.   Junior, E.G.S., et al., *Biodiesel production from heterogeneous catalysts based K2CO3 supported on extruded γ-Al2O3.* Fuel, 2019. **241**: p. 311-318.

62.   Ruppel, T., T. Huybrighs, and C. Shelton, *Fatty acid methyl esters in B100 biodiesel by gas chromatography (Modified EN 14103).* Application Note, Perkin Elmer, 2008. **2012**.

Appendix A

Methanol to oil ratio calculation

This work used methanol to oil ratio of 15:1 for transesterification reaction. The calculation was followed by this example.

Example:

$$\frac{Mole\ of\ palm\ oil}{Mole\ of\ methanol} = \frac{1}{15}$$

$$\frac{Mole\ of\ palm\ oil}{MW.\ of\ palm\ oil} \times 15 = \frac{Mass\ of\ methanol}{MW.\ of\ methanol}$$

$$Mass\ of\ methanol = 15 \times \frac{100}{851} \times 32.04$$

$$Mass\ of\ methanol = 56.48\ g$$

when   Mass of palm oil is 100 g.

The methanol to oil ratio is 15:1.

Molecular weight of methanol is 32.04 g.

Molecular weight of palm oil is 851 g.

Appendix B

The percent of methyl ester calculation

The %FAME was calculated, following the EN14103 standard method. Methyl heptadecanoate was used as internal standard [62].

%FAME can calculated follow below equation:

$$C = \frac{\sum A - A_{EI}}{A_{EI}} \times \frac{C_{EI} \times V_{EI}}{m} \times 100$$

when C is the percent of methyl ester

$\sum A$ is total area from $C_{12} - C_{24}$

A_{EI} is area of methyl heptadecanoate

C_{EI} is concentration of methyl heptadecanoate solution (mixed with heptane, mg/mL)

V_{EI} is volume of methyl heptadecanoate (mL)

m is mass of biodiesel sample (mg)

Example: FAME area from the batch which use 40TSP/ACBT

$$\sum A = 4077297.948$$

$A_{EI} = 667724.875$

$C_{EI} = 10.023$ mg/mL

$V_{EI} = 1$ mL
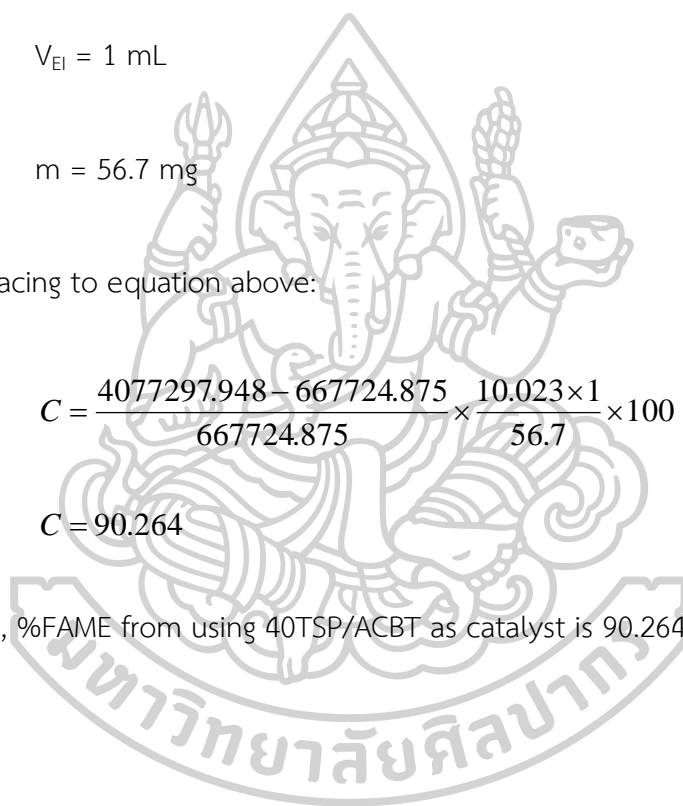
m = 56.7 mg

Replacing to equation above:

$$C = \frac{4077297.948 - 667724.875}{667724.875} \times \frac{10.023 \times 1}{56.7} \times 100$$

$$C = 90.264$$

Thus, %FAME from using 40TSP/ACBT as catalyst is 90.264%
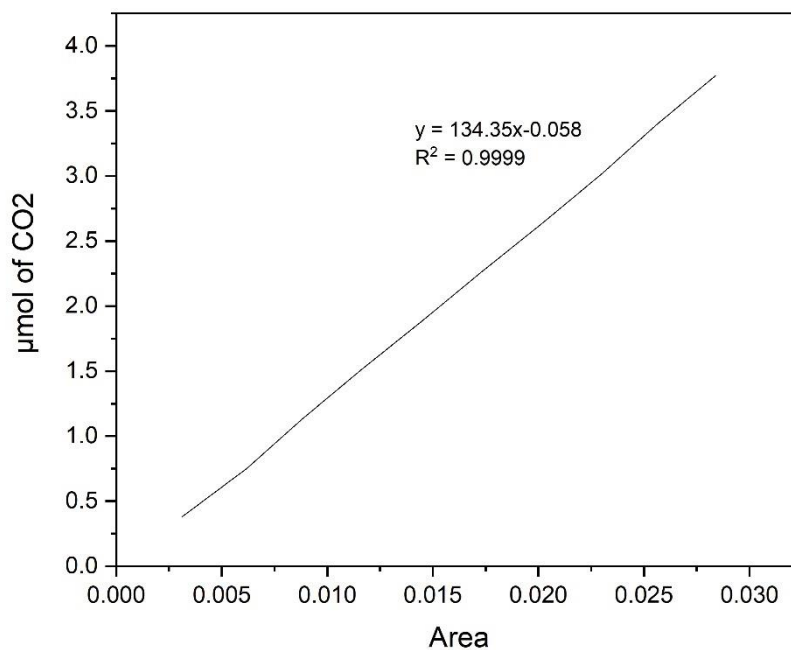
Appendix C

The basic site calculation

Figure 38 *Calibration curve of CO_2*

The calibration curve was plotted using CO_2 injection which varied volume from 10-100 μL. After the injection, the area in various value occurred. The volume of CO_2 injection was converted into mol CO_2 using ideal gas equation. The graph was plotted between area and mol of CO_2 as seen in Figure 38.

The result of CO_2-TPD was presented in the form of area. The equation in Figure 38 was used to calculate mol of CO_2 by replacing x with the area from CO_2-TPD result.

Example: Find basic site of 40TSP/ACBT

CO_2-TPD area is 2.95.

Weight of characterized catalyst is 0.1061 g.
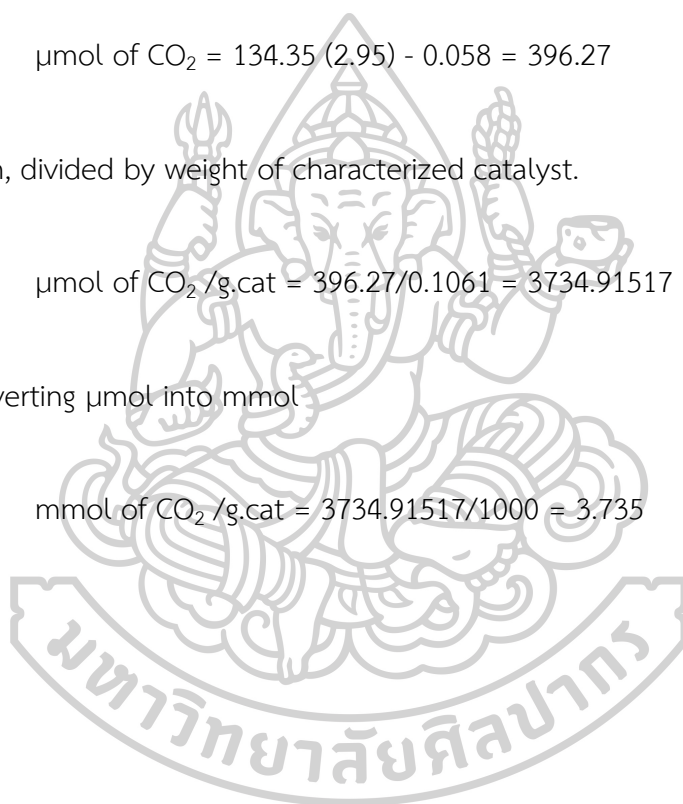
μmol of CO_2 = 134.35 (x) − 0.058

μmol of CO_2 = 134.35 (2.95) - 0.058 = 396.27

Then, divided by weight of characterized catalyst.

μmol of CO_2 /g.cat = 396.27/0.1061 = 3734.91517

Converting μmol into mmol

mmol of CO_2 /g.cat = 3734.91517/1000 = 3.735

VITA

NAME   Teerapat Hasakul

DATE OF BIRTH   3 January 1996

PLACE OF BIRTH Pahonpholpayuhasena hospital

HOME ADDRESS   2/97 Village No.5, Sangchuto road, Thamakham, Mueang

Kanchanaburi, Kanchanaburi 71000